Title

Cognitive dysfunction and anxiety resulted from synaptic downscaling, hippocampal atrophy and ventricular enlargement in i.c.v. streptozotocin injected male Wistar rats

Authors

Avishek Roy[1], Sakshi Sharma[2], Tapas Chandra Nag[3], Jatinder Katyal[4], Yogendra Kumar Gupta[5], Suman Jain[1]

Affiliations

[1]Department of Physiology, All India Institute of Medical Sciences, New Delhi; [2]Humanities and Social Sciences, Indian Institute of Technology, New Delhi; [3]Department of Anatomy, All India Institute of Medical Sciences, Delhi; [4]Department of Pharmacology, All India Institute of Medical Sciences, New Delhi; [5]Translational Health Sciences and Technology Institute, Delhi.

Abstract

Intracerebroventricular streptozotocin (ICV-STZ) injection is among the best animal models to simulate sporadic Alzheimer's disease (AD) (Hoyer, 2002, 2000, 1998; Salkovic-Petrisic and Hoyer, 2007). Brain insulin signaling abnormality (Grünblatt et al., 2007), neurodegeneration (Kamat, 2015), neuroinflammation (Liu et al., 2022), cholinergic damage (Blokland and Jolles, 1993; Roy et al., 2021), mitochondrial dysfunction (C. Correia et al., 2013), genetic abnormality (Chen et al., 2012), respiratory problem (Ebel et al., 2017), oxidative stress (Sharma and Gupta, 2001), gliosis (Rostami et al., 2017), sleep disturbances (Song et al., 2018) associated with cognitive abnormalities seen in ICV-STZ injected rats. Available experimental evidences has used varying doses of STZ (<1 to 3mg/kg) and studied its effect for different study durations, ranging from 14-21 (short), 30-42 (mild), 90-105 (moderate) and 250-270 (long) days (Chen et al., 2013, 2012; Grünblatt et al., 2007; Knezovic et al., 2015; Kraska et al., 2012; Mehla et al., 2013; Rostami et al., 2017; Salkovic-Petrisic et al., 2006). These studies indicated that 3mg/kg of body weight is the optimum dose for inducing sporadic AD in the rodents. However studies on the pathological process with relating the morphological and functional abnormalities reported were illusive.

Therefore in the present study, we have investigated the effect of 3mg/kg ICV-STZ on three cognitive domains viz. spatial, episodic and avoidance and even neuropsychiatric abnormality i.e. anxiety with extensive morphological examination in the layers associated with hippocampus proper. Further, we have observed the onset of diffuse amyloid plaques, in association with enlargement of lateral ventricles and down scaling of spines in granular cells of dentate gyrus. Finally, to dissect the functional changes in spatial and anxiety variables we had examined the probability of fraction of time spent in Morris water maze and changes in ethological patterns of STZ injected rats in elevated plus maze.

Introduction

AD is one of the commonest form of dementia in the world, which is characterized by the deposition of hyperphosphorylated tau, amyloid beta (Aß) in cerebral parenchyma which is tightly associated with cognitive impairment. Further, cognitive impairment in AD is reported to be resulted due to synaptic dysfunction and loss of adult neurogenesis, one of the intrinsic property of brain to regenerate at adulthood. On the other hand, insulin resistance is the gold standard for early detection of AD in patients using imaging viz. FDG-PET. ICV-STZ injection is reported to have a pathology like sporadic AD through similar process. Varied doses with different time period for studying the pathological events after STZ injection is available. Those studies indicated 3mg/kg to be the best choice for inducing the sporadic AD in rodent,

in terms of progression in cognitive decline, and this was associated with manty micro and macro structural changes ranging from mitochondrial dysfunction to cortical thinning. However, relevant studies were not available deciphering the morpho-functional pathological processes after 3mg/kg ICV-STZ injection. When we had categorized previous studies with different time-periods like short, moderate, long then we have seen that, short duration studies showed cognitive impairment, anxiety, hp-tau deposition, neurodegeneration, and gliosis on 14th, whereas GSK3ß increment in hippocampus on 30th day after STZ injection (Chen et al., 2013; Salkovic-Petrisic et al., 2006). Further, these phenotypes were observed due to cellular, mitochondrial and insulin dysfunction of brain(C. Correia et al., 2013). However, moderate studies revealed increase in $Aß_{1-42}$ and amyloid plaque deposition, expression of AKT/PKB, expression of insulin1&2-mRNA and IR in hippocampus and frontoparietal cortex on the 80-90th day with a trend for reversal from acute cognitive impairment on 14th day (Grünblatt et al., 2007; Rostami et al., 2017; Salkovic-Petrisic et al., 2006). Long temporal observations have shown disturbance of avoidance memory following a biphasic pattern, with insult to parietal cortex and corpus callosum(Knezovic et al., 2015). Apart from dose-response studies, other studies on the ICV-STZ model showed role of novel drugs in sporadic model of AD viz. antia (El Sayed and Ghoneum, 2020), PPAR agonist (Lin et al., 2022), QTC-4-MeOBnE (Fronza et al., 2019), magnesium (Xu et al., 2014) etc. Whereas in another two sequential papers ICV-STZ has been compared to 3xTg model of familiar AD, where authors has reported to have altered expression of 84 genes related to APP processing, apoptosis, mTOR and insulin signaling, and also impairments in episodic memory, anxiety, and no change in motor activity or related postural balance after unilateral injection of 3mg/kg ICV-STZ in female mice at 42nd day post injection (Chen et al., 2013, 2012). Whereas in another more recent study by Bao et al., 2017 reported differences in the effect of ICV-STZ in cognitive as well as neuronal morphometry tightly associated with sex specificity in Sprague-Dawley rats. More specifically, female rats responded less to the toxicity of STZ in comparison to male counterpart and authors has showed role of estradiol in such changes (Bao et al., 2017). In one paper by Gaspar et al., 2021 interestingly reported that ICV-STZ exerts no significant cognitive impairments in comparison to control counterpart, which suggest that selection of strain has importance in modeling human disease in animals (Gáspár et al., 2021).

Therefore, in the present study we had used male Wistar rats purposefully to decipher the pathological downstream in terms of behavioral and morphological changes in the best suggested drug dose for inducing sporadic AD i.e. 3mg/kg. To do so we have first followed up the spatial, episodic, avoidance memory and anxiety level simultaneously at a interval of 15 days till two months period. At the end of the study period we have validated our behavioral findings with the morphometry, volume analysis on cresyl violet stained samples and synaptic morphometry on Golgi-Cox stained samples. Next, amyloidopathy, insulin signaling, mitochondrial dysfunction if any was examined by congored staining or immunofluorescence in brain areas of limbic system. Finally in the current paper apart from the regular analysis of behavioral data we have further looked at the distribution of fraction of time spent on 60th day probe trial in MWM and ethograms of animals on 60th day in EPM in order to dissect the functional changes in cognitive and neuropsychiatric domain.

Materials and Methods

Animals:

Total 54 male Wistar rats (280±10gm) were included in the present study, which are maintained in standard housing conditions at an ambient room temperature of 25±1ºC, relative humidity of 50-55% and the light-dark cycle of 14:10 hr. Rats were provided with *ad libitum* access to food and water, each housed individually in polypropylene cages (50cmX20cmX15cm) with

metallic lid, which has separate laboratory chow and water bottle holders. All precautions were taken during the period of housing to avoid pain. All the experimental protocols were approved by institutional animal ethical committee (*file no. 937/IAEC/PhD-2016*), in accordance with committee for the purpose of control and supervision of experiments on animals (CPSCEA) guidelines.
Rats were randomly divided into three groups viz. Control, Sham and AD. Where Sham and AD group of animals were injected with artificial cerebrospinal fluid (aCSF) or STZ respectively in the lateral ventricles. Among the 18 rats recruited in each group 16, 15 and 12 rats were survived till the end of the study period in Control, Sham and AD group respectively. Therefore, total survival rate in all experimental groups are 68%; furthermore mortality rate in 3mg/kg STZ injected rats were up to 33.33% in the present study. For behavioral experiments we have used ≥9 animals, for histological and biochemical experiments we have recruited 3 and 4 animals/ group.

Experimental design:
After adaptation to the departmental animal facility, rats were randomly divided into three groups using block-size randomization (Efird, 2011):

Control:	age matched cage control animals housed in same condition to others
Sham:	5µl/site bolus injection of aCSF bilaterally at lateral ventricles
AD:	3mg/kg of b/w bolus injection of STZ bilaterally at lateral ventricles

Primarily, all baseline behavior was recorded for all the experimental groups within first week after adaptation period to the colony room. Next, groups were homogenized based on baseline behavioral data in order to avoid any baseline bias. And animals were undergone surgery for Sham/ AD group with aCSF/STZ respectively. From then animals were tested for their cognitive and non-cognitive behaviors at a interval of 15 days for a stretch of two months. At the end of the study period animals were sacrificed either via transcardial perfusion or CO_2 concussion for histological and biochemical experiments respectively.

Behavioral assessments:
In present study, Morris water maze (MWM), one trial object recognition (OTORT), step-down passive avoidance (SDPA) and elevated plus maze (EPM) tests were chosen for spatial reference, episodic recognition, avoidance memory and unconditioned anxiety due to fear of height respectively. All behavioral assessments were recorded and analyzed with video tracking devices except for passive avoidance test, which was conducted manually. Behavioral execution in cognitive and non-cognitive tasks were recorded on 15th, 30th, 45th and 60th day post-injection of aCSF/STZ accordingly.

Morris Water Maze test:
Morris water maze test was conducted to decipher reference spatial memory in the experimental animals as described previously (Mehla et al., 2012a; Morris, 1984). In MWM a water tank (metallic, customized, 170cm dia. X 72cm height) has been divided into four equal imaginary quadrants with the help of video-tracking software. Animals were trained to remember how to escape swimming by entering onto hidden platform (10cm dia. X 35cm height). The hidden platform was situated in fourth quadrant for two minutes in consecutive four days, where fourth quadrant was refereed with an intra-maze cue. A training trial was started by placing the animal facing towards wall of the tank. Trial was terminated once animal sit on the platform for 10 second or 120s elapsed, whichever condition meet first. If animals

did not reach destiny on time then they were manually guided to the platform by the experimenter.
On the fifth day, a spatial probe trial was conducted where protocol was same as mentioned in previous paragraph except animals were allowed to explore the tank only for 60s and and no platform has been placed inside the tank. All the trials has been recorded and data has been acquired using AnyMaze software (ver.05; Stoelting Corp., USA). Furthermore, only probe trial was repeated on the follow-up days post-injection for retention of spatial memory.

Dirichlet distribution of swimming strategy in Morris water maze:
Dirichlet distribution is a multivariate generalization of beta distributions. Where in the recent paper it has been used a stand-alone test to determine whether the animals spend the same time in the four imaginary quadrants of MWM tank (Maugard et al., 2019). Four quadrants were conceptualized as one target quadrant (TQ), one opposite quadrant (OQ), and two alternative quadrants (AQ). Where hypothesis of the statistical model has been raised as null hypothesis will be considered once fraction of time spent in TQ=AQ=OQ. Further, for understanding the outcome authors has proposed a new way to plot the data from the four quadrants as the aforementioned conceptions, where graph will show mean values and inter-individual variability at the same time, on an easily interpretable chart. For the analysis we have used code available at https://github.com/xuod/dirichlet.

One trial object recognition test:
The open field was used to conduct one trial object recognition test according to (Ennaceur and Delacour, 1988), which specifically target episodic memory. Wooden/metallic/glass/plastic objects with different shapes and sizes, they are of primary colors with different palpable textures were tested for their 'interest index' a parameter assessed for ability to induce interest for novelty (data in supplementary fig.S1.a.); however in the present study plastic/glass made objects were used in the present study.
In OTORT animals were first habituated with a open field arena (50cm X 50cm, Coulbourne Instruments, USA) with an exploration time of 5min two times/day for 3 days. On the fourth day, a 'sample phase' was conducted where animal was placed in the center of the arena facing towards wall with similar objects at a same distance from the wall (10cm from the wall). With a delay of fifteen minutes of 'sample phase' animals were allowed to explore the same arena for 5min, except one of the sample object is being changed with a novel one. This phase is called 'test phase'. We have chosen fifteen minute time gap between two phases to target short term memory. In both these phases exploration of the animals were tracked with CCD camera (Panasonic, Japan) using Ethovision XT (ver. 07, Noldus Co., Netherlands) and data acquired and analysed for recognition and discrimination index. Formulae are as follows:

- Recognition index= {(time spent exploring novel object)-(time spent exploring familiar object)}/{(time spent exploring novel object)+(time spent exploring familiar object)}
- Discrimination index= {(time spent exploring novel object)-(time spent exploring familiar object)}/{(time spent exploring novel object)+(time spent exploring familiar object)}

On the follow-up time periods at an interval of 15days 'test phase' was repeated.

Stepdown test for passive avoidance:
Passive avoidance was tested in rats to assess long-term avoidance/fear memory deficits in accordance with (Filho et al., 2015). We have used modular animal test cage with metal grid floor which is part of Skinner Box (model:E10-10SF, Coulbourne Instruments, USA), this was connected with an animal test cage grid floor shocker (model:E13-08, Coulbourne Instruments,

USA) with a safe bench/ wooden platform where animals were placed before starting the experiment. We have used 'consolidation protocol' consisting a training phase, and 24hr later a test phase. On training phase, rat was placed onto the safe bench and upon stepping down to grid floor with its four limbs it got an electric shock of 2mA for 3s. Retention of memory was defined as avoiding foot shock by not being active on grid floor on second day/test phase. After 24hr of training phase same protocol was followed except foot shock upon step-down and behavior was observed for 3 minutes of time. In this observation period number of step down (errors) and latency to the first step down on the grid floor was measured manually.
We have repeated the second day/ test phase on every 15 day interval of post-injection of STZ in the experimental groups and same parameters were recorded as a measure of retention of fear memory.

Elevated plus maze test:
Elevated plus maze (EPM) paradigm was conducted in order to decipher the anxiety like behavior, and this in accordance with previous method (Walf and Frye, 2007). This behavior is based on the anxiety induced by the fear of height in rodents. We have used an EPM setup consists of a customized plus maze with an opaque plastic board fixed on to iron frame made out of plywood. The length of the open and closed arm of 76cm and 134cm respectively, with a junction of arms i.e. central area of 6X6cm. Animal's behavior was video tracked with CCD camera (Panasonic, Japan) associated with Ethovision XT (Ver. 07, Noldus, Netherlands). We have conducted one day protocol with a prior habituation of the animal to the behavioral testing room for minimum 30min and then animals were placed in the central area of the EPM facing either side of the open alley. And then animals were allowed to explore the arena for 5min.
Lastly, in the EPM test animals were placed on the central zone facing towards open arm and allowed to explore for five minutes, while time spent and head dipping was recorded. The same was followed in the follow-ups.

Behavioral scoring with kinoscope for elevated plus maze:
Apart from the regular analysis of the quantitative variables for elevated plus maze test from the video tracking software (i.e. Ethovison XT), we also performed post-hoc behavioral scoring from the video tracked by a separate researcher blind to the experiment (intra rater reliability ≥ 0.9). This is being performed using an available algorithm program 'kinoscope' (Kokras et al., 2017) where manually behavioral execution was coded using specific key tagging for different ethograms (viz. exploration to five zones, unprotected head dip etc.), and visual maps were graphically depicted corresponding to individual animals to get an idea about the intra-group variability. These maps of events from start to the end of paradigm (i.e. 0th to 300th seconds) were coded with specific color.

Selection of dose and stereotactic coordinate for injection of streptozotocin:
In order to select the dose of streptozotocin to be used in the present study we have performed a separate experiment involving three groups mentioned here 5 animals/group. Where AD group animals were injected with three separate doses of STZ viz. 1.5mg/kg; 2mg.kg; 3mg/kg at the lateral ventricles as mentioned in the following section. And then the animals were tested for cognitive and anxiety like behavior for 45 days and at the end neurodegeneration in the brain sections were examined by cresyl violet staining. Our observation showed that 3 mg/kg dose is best suited for studying the disease progression for a chronic time period (see supplementary fig. S1.b.).
On the other hand, for selection of stereotactic coordinates we have used three separate coordinates and Chicago blue dye was injected using the stereotactic guiding setup (David Kopf, USA), where we found AP: -0.84mm; ML: ±1.5mm; DV: -3.5mm as the best choice for

the reason that it has good breathing space for surgical manipulation. Which gives researcher a robust coordinates for same precision each time (see supplementary fig. S1.c.).

Intracerebroventricular injection in rats:
In order to induce Alzheimer's disease or to prepare sham operation intracerebroventricular injection of streptozotocin (STZ; 3mg/kg of b/w; bilateral) or artificial cerebrospinal fluid (aCSF; 5µl/site; bilateral) treated respectively by stereotaxic manipulation under sodium thiopentone (50mg/kg of b/w) anesthesia. Injection was given using a 25µl Hamilton syringe (22G; 700N glass) placed in arm-held Elite-11 mini pump (Harvard Apparatus, USA) at a rate of 1µl/min while body temperature was maintained during and after surgery in homeothermic monitoring system (Harvard Apparatus, USA) following previous protocol (Ferry et al., 2014). Briefly, after anesthesia animals were fixed in David-Kopf stereotaxic frame and flat-skull position was cross-checking DV position of Bregma and Lambdoid suture, finally injection was given at AP: -0.84mm; ML: ±1.5mm; DV: -3.5mm coordinates through a burr-hole made using a drill-bit (>22G) attached to driller (Foredom, USA). After completion of each injection needle was kept in the same position at least for 3min. Further, postoperative care was taken using meloxicam (Intas pharmaceuticals, India); and gentamycin (Neon Laboratories, India) as analgesic and antibiotic respectively for 3-5 days. aCSF was prepared as reported previously (Mehla et al., 2012a). Furthermore, after preparation of aCSF it was checked for osmolality in order to avoid any osmotic shock in the brain with vapour pressor osmometer (5600; Vapro; Wescor Inc.; USA).

Transcardial perfusion and tissue harvesting:
At the end of the study period animals were subjected lethal dose of anesthesia and then tissues were collected and proceeded for histological examinations as follows:
On the 60th day followed by terminal behavioral assessments animals were subjected to 150mg/kg of sodium thiopentone (i.p.) without any anti-cholinergic drug. After confirmation of complete anesthesia by paw-pressor, animals were placed onto a ice-pack on its back and immediately a lateral incision was made integument and abdominal wall and then small incisions were made to access the plural cavity by through incising diaphragm and cardiac envelop was excised to access heart as mentioned the previous protocol (Gage et al., 2012). Finally, preceding with ice-cold saline (0.9%NaCl; W/V), ice-cold PFA (4%, W/V) was perfused at a volume of 50-60ml transcardial. Furthermore, brain was then dissected out by decapitation avoiding damage to the tissue and post-fixed in the same fixative for 3-4day (2-8°C). Next, after separating the cerebellum, tissue was cryo-protected with graded sucrose solution (15% and then 30%; W/V in 1X PB). Finally, 20µm thick coronal sections were taken onto gelatin (3%; w/v; Sigma Aldrich) coated slides using cryo-stat (Microm HM550; Thermo Scientific). Sections were kept at 2-8ºC until used further.

Histology
To examine cytoarchitecture, the sections of the brains were stained only with cresyl violet (Nissl stain) following a standard protocol as follows. After 2min clearing with xylene samples were dehydrated with absolute alcohol for 2 min. Next, sections were treated with graded alcohol with decreasing order (95% and then 75%), following an incubation in alcohol: chloroform solution (40:60, v/v) for 1min in room temperature. Then, sections were incubated with Cresyl violet stain (0.4% in MiliQ; CDH, India) for 3min in room temperature (RT) followed by a hydration with distilled water. After that, dehydrated with graded alcohol in increasing order (75% and then 95%). Then, treated with 1-N butyl alcohol for 1 min in RT followed by a 1 min treatment with alcohol: chloroform mixture (40:60, v/v). Finally, sections were cleared two times with xylene solution and mounted with DPX (Merk Ltd., India).

Separately, congored (Sigma Aldrich, USA) staining was performed to assess amyloid plaque using previous protocol with some modifications (Bott, 2014) with counter staining with haematoxylin for nucleus. For hippocampal section histometric comparison between groups in different study period we have restricted to AP-axis from -3.48 to -3.71 mm following rat brain atlas (Paxinos and Charles Watson, 2007). Furthermore, stained sections were kept in dark at RT until imaging.

Golgi-Cox staining

In order to investigate the neurite complexity in the dentate gyrus of the dorsal hippocampus we have performed Golgi-Cox staining modified from two previously reported protocols (Ranjan and Mallick, 2010; Zaqout and Kaindl, 2016). After terminal behaviour testing brain was dissected followed by euthanasia and 5mm chunk of dorsal hippocampus using brain matrix (51388, Stoelting Co., USA) was incubated in Golgi-Cox solution at 37ºC for 24hr. Next, sections were made pliable with sucrose solution (30%, W/V in PB) in 2-8ºC for 2 days. Then, 200µm thick section was made using vibratome (VT1000S, Leica, GmbH) from chunk embeeded in agar (3%, W/V in PB). After taking sections on to gelatine (Sigma Aldrich, 3%, W/V in MQ) coated slides and proceed to development and finally mounted with DPX (Merk Ltd., India). Further, stained sections were kept in dark before imaging.

Immunostaining

For immunolabeling of the sections, first sections were hydrated with PBS (1X) for 5min in RT and next penetrated/ permeabilized with PBST (0.2% Tween-20 in PBS, v/v) for 5min in RT. Next, sections were blocked with BSA (1% in PBST, w/v) for 2hr in RT before incubated sections with anti-GSK3β (1:400; ITT05016, Immunotag, USA), anti-mtCOX (1:200; 1D6E1A8, Abcam, USA), anti-PI3K (1:500; ITT03242, Immunotag, USA) separately for 2days at 2-8ºC in refrigerator. After incubation with primary antibody, three times wash with PBS was given for 5min each at RT. Next, sections were incubated with specific secondary antibody accordingly viz. anti-rabbit (1:400; DI-1594; vector laboratories, USA), anti-mouse (1:1000; fl-2000; Vector laboratories, USA) for 2hr. Finally, sections were mounted with fluoroshield with DAPI (F6057, Sigma Aldrich, USA), followed by a wash with PBS for three times for 5min each at RT. Finally, stained sections were kept in dark at 2-8ºC until imaged using fluorescence microscopy.

Image acquisition and its analysis

Brain sections stained with dye viz. cresyl violet, congored, Golgi-Cox were imaged using the brightfield condition available in the Eclipse Ni upright microscope equipped with motorized (driver remoted) platform (Nikon, Japan) using an empty filter (dicroic mirror 0-∞) with an auto-white filter in the area where sections are not present. For fluorescence imaging same microscope was used additionally with fluorescence intensilight lamp (C-HGFI, Nikon, Japan) where we have used triple filter block of DAPI (blue; excitation at 385-400nm; bandpass at 393CWL) FITC (green; excitation at 475-490nm; bandpass at 483CWL) and TRITC (red; excitation at 545-565nm; bandpass at 555CWL) according to the need. Camera setting were optimized to achieve best image with less photobleaching. All the images in this paper were captured using a colour camera to the microscope (DSRi-2; Nikon; Japan) and saved in RGB format for further use.

Images of cresyl violet, Golgi-Cox and immune stained sections were analysed for histometric and morphometric evaluations. In case of the counting of the number of viable cells and its soma area we have used a specific workflow in the NIS Element basic research software (Nikon, Japan) platform (see supplementary fig.S1.d.). One the other hand variables viz. lateral ventricular volume, layer wise volumetric measurement, and immune-positive signals were

measured/ counted, neurite length, spine density using 'line tool' or 'multi-point tool' in the FIJI software (Schindelin et al., 2012). All the measurements were done in the 400X magnified images, this was strictly maintained to have appreciable observation of the signals. Cell/ signal counting results were normalized and plotted as 'per unit area'.

Statistical analysis

For data distribution, Shapiro-Wilk normality test was performed. Sample size were kept as per previous reports. For the within group comparison of behaviour with follow-up one-way ANOVA (non-parametric, two tailed, repeated measures) was performed with Bonferroni's correction for multiple comparison. For comparison between two groups t-test (nonparametric, Mann-Whitney, two tailed) was performed. For cell count, area of the viable cell and subcellular localization, we have performed one-way ANOVA (non-parametric, two tailed, ordinary). These aforementioned statistics were performed in Prism 8.0 (GraphPad Software Inc, San Diego, CA). Distribution of swim-time in the four quadrants were analyzed using a continuous multivariate probability distribution named Dirichlet distribution using a python pipeline. On the other hand, the ethograms in EPM test were analyzed and plotted using a specific algorithm named Kinoscope. We have performed pairwise correlation of the dataset in case of understanding morpho-functional relationship. A p-value of ≤ 0.05 was considered significant and data was shown as individual values with mean and standard error of mean. Otherwise, data were shown with only mean and standard error of mean.

Results

Spatial memory impairments after streptozotocin treatment

In the latency to the goal quadrant, we found a significant effect of time ($p<0.0001$; df= 2; F=20.72), treatment ($p<0.0001$; df= 4; F= 10.00) as well as the interaction between both of them (p= 0.0021; df= 8; F= 3.261). Further, on multiple comparisons, latency was found to be increased significantly on 15th day (p= 0.0222), 30th day (p= 0.0002); 45th day ($p<0.0001$), and 60th day (p= 0.0001) in AD group when compared with its baseline. In the time spent in goal quadrant, two- way ANOVA revealed only significant effect of treatment ($p<0.0001$; df= 4; F=12.37) and interaction between time and treatment (p= 0.0043; df=8; F= 2.992). Bonferroni's multiple comparison showed significant reduction of time spent in goal quadrant in sham group on 15th day (p= 0.0027) and 60th day (p= 0.0013) with respect to its baseline, whereas, in AD group, it was reduced on 15th day (p= 0.0028), 30th day ($p<0.0001$), 45th day ($p<0.0001$), 60th day ($p<0.0001$) when compared with its baseline. In the number of entries to the goal quadrant, only treatment was shown to effect the results significantly (p= 0.0048; df= 4; F= 3.943). Further, on multiple comparison AD group of rats had significantly less number of entries/ visits to the goal quadrant on 30th day (p= 0.0361) and 60th day ($p<0.0001$) (fig. 1.A-C.).

On analysis of the latency to the platform zone, we observed only treatment to affect significantly the results (p= 0.0005; df= 4; F= 5.401). Multiple comparison analysis revealed a significant increase in latency to the platform zone on 60th day in sham (p= 0.0211) and AD (p= 0.0007) group when compared with their baseline. In case of time spent in platform we found both time (p= 0.0006; df= 2; F= 7.859) and treatment ($p<0.0001$; df= 4; F= 8.292) to be significantly different. When multiple comparison was conducted, we observed a decrement on 15th day (p= 0.0202), 30th day ($p<0.0001$), 45th day ($p<0.0001$), 60th day ($p<0.0001$) in comparison to baseline in AD group only. Number of entries to the platform zone was found to be influenced significantly by treatment ($p<0.0001$; df= 4; F= 8.660) and multiple comparison test revealed a significant decrement on 30th day (p=0.0006), 45th day (p= 0.0004), and 60th day (p= 0.0001) in AD group when compared to its baseline (fig. 1.D-F.).

Next, in order to understand the changes between group at different experimental follow-ups we performed Kruskal-Wallis test with Dunn's multiple comparison on latency to the goal quadrant. Statistical analysis revealed no significant mean difference across the groups at baseline pre-surgery data (p= 0.35, df= 2, KW= 2.07). However, Kruskal-Wallis test showed a significant mean difference at 15th day (p<0.0001, df= 2, KW= 32.02), 30th day (p<0.0001, df= 2, KW= 27.34), 45th day (p<0.0001, df= 2, KW= 30.30) and 60th day post-injection of STZ(p<0.0001, df=2, KW= 30.33). Dunn's multiple comparison on each day revealed a significant increase in AD group as compared to Control (p<0.0001) and Sham (p≤ 0.01) (fig. 1.G.). Furthermore, occupancy plot of control and the sham operated groups showed a red or yellowish red in the platform zone respectively, whereas in case of AD group it was found to be blue (fig. 1.I.i-iii.; left panel).

Distribution of swimming time in the four quadrants of Morris water maze

In order to probe the strategic changes in the spatial reference memory after i.c.v. STZ injecti on in the lateral ventricles, we performed likely-hood ratio statistics (LRS) based on Dirichlet distribution. On 60th day post-injection of STZ, analysis of fraction of time spent in the each quadrant was looked for uniformity within group. Results found a significant uniform distribu tion in Control (p= 7.88896e-17; LRS= 78.0884), Sham (p= 4.74448e-14; LRS= 65.113), exc ept in AD (p= 0.473182; LRS= 2.51169) group. Furthermore, as in this statistics we considere d equal time spent in each quadrant as null hypothesis (H0) and the alternative hypothesis (H1) was that at least one quadrant will differ significantly. Hence, analysis showed that H0 was t rue only for Control and Sham group of animals (fig. 1.I.i-iii.; right panel). These finding sug gests that, i.c.v. STZ injected rats on 60th day post-injection uniformly spent fraction of the s wimming time in the MWM tank. This behavioural change directly reflect an impairment in l ong term memory loss on the very follow-up day.

Recognition memory deficits after streptozotocin treatment

When we applied repeated measures two way ANOVA on the recognition index with post hoc Bonferroni's multiple comparison test, a significant effect of treatment (p<0.0001; df= 4; F= 16.20), time (p<0.0001; df= 2; F= 168.4) and even interaction between the two (p<0.0001; df= 8; F= 13.19) was observed. On multiple comparison between time points, in AD group of rats only, a significant reduction of recognition index on 15th (p<0.0001), 30th (p<0.0001), 45th (p<0.0001), and 60th day (p<0.0001) was evident in comparison to its baseline (fig. 2.A.). In addition, intragroup analysis of discrimination index showed a significant effect of treatment (p<0.0001; df= 4; F= 17.74), time (p<0.0001; df= 2; F= 184.4) and even interaction (p<0.0001; df= 8; F= 14.44). Multiple comparison showed a significant decrease in AD on 15th (p<0.0001), 30th (p<0.0001), 45th (p<0.0001), and 60th day (p<0.0001) as compared to its baseline (fig. 2.B.).

Furthermore, a significant change in recognition index among the experimental groups examined on 15th day (p= 0.0014; df=4; F= 11.87), 30th day (p= 0.0002; df= 4; KW= 17.51), 45th day (p= 0.0001; df= 4; KW= 18.21), and 60th day post-surgery (p= 0.0005; df= 4; KW= 15.34). No significant difference among the groups was evident at baseline (p= 0.775, df= 4, F= 0.508). Post hoc multiple comparison revealed a significant decrease of recognition index in AD group as compared to the Control (p<0.0001) and sham operated (p≤0.003) groups on all the follow-up days (fig.2.D.). Similarly, between group analysis of discrimination index showed no significant difference among the groups at their baseline (p= 0.775; df= 4; KW= 0.508). However, a significant change was observed on post-surgery day 15 (p= 0.0014; df= 4; F= 11.87), 30 (p= 0.0002; df= 4; KW= 17.51), 45 (p= 0.0001; df= 4; KW= 18.21), and 60 (p= 0.0005; df= 4; KW= 15.34). Moreover, multiple comparison revealed significant reduction

of discrimination index in AD group as compared to Control ($p \leq 0.001$) as well as Sham ($p \leq 0.003$) group at all time points (fig.2.E).

Representative track-plots of the of the Control and sham groups on 60th day test phase showed more number of line crossing of the nose point (cyan colour), directed/ headed towards novel object in comparison to the familiar one. However, in AD group it was directed towards familiar object, which confirms the results of recognition and discrimination index described in aforementioned paragraph (fig. 2.C.).

Avoidance memory impairments after streptozotocin treated rats

After training for PASD task at baseline, all the rats were tested for retrieval of avoidance memory following STZ injection at an interval of 15 days till 60 days to decipher progression of the disease. Within-group analysis using repeated measures two-way ANOVA with Bonferroni's multiple comparison test on the latency to the step down revealed a significant influence of interaction between the two ($p<0.0001$; df= 8; F= 110.1), treatment ($p<0.0001$; df= 4; F=178.5), and time ($p<0.0001$; df= 2; F= 1737). Further, post-hoc analysis showed a significant decrease on 45th (p= 0.0169) and 60th day (p= 0.0004) in Sham, and in AD the decrease was significant ($p<0.0001$) from 15th until 60th day as compared with their baseline (fig. 3.A.).

Within-group analysis of number of errors at different time-points showed only a significant influence of time (p=0.0220; df=2; F=3.939), and comparison with Tukey's multiple comparison test showed significant increase in number of errors in AD group on 60th day (p=0.0087) as compared to its baseline (fig. 3.B.).

However, between group analysis failed to show any significant mean differences across the group at baseline (p= 0.75), but post-STZ injection, we found a significant change between the groups examined on 15th ($p<0.0001$, df= 2; KW= 19.25), 30th ($p<0.0001$, df= 2, KW= 17.79), 45th (p= 0.0002, df= 2, KW= 17.51) and 60th day (p= 0.0001, df=2, KW= 18.00). Further, multiple comparisons revealed significant reduction in AD group versus Control ($p \leq 0.001$) and Sham ($p \leq 0.01$) group of rats (fig. 3.C.).

Neuropsychiatric effects seen in streptozotocin treated rats

On analysis of ratio of time spent in open vs closed arm, we observed time (p= 0.0003; df= 2; F= 8.829) to have a significant influence on the results. However, following multiple comparison, no statistically significant changes with time in any of the groups was observed (fig.4.A.). In head dipping duration, within-group analysis showed a significant influence of treatment (p= 0.0002; df= 4; F= 5.936), time ($p<0.0001$; df= 2; F= 55.82) as well as interaction between the two factors (p= 0.0096; df=8; F= 2.680). Further, multiple comparison revealed reduction in duration of the head dipping in AD group on 30th (p= 0.0032), 45th (p= 0.0057) and 60th day (p= 0.0001) as compared to its baseline (fig.4.B.).

Kruskal-Wallis test for comparison of data between the groups revealed no significant difference between groups at baseline (p= 0.93, df= 2, KW= 0.13), on 15th (p= 0.095, df= 2, KW= 4.7), 30th day (p= 0.18, df= 2, KW= 3.41) and 45th day (p= 0.12, df= 2, KW= 4.08). Only on 60th day a significant difference was observed (p=0.0022, df= 2, KW= 12.25) across the groups. Further, Dunn's multiple comparison revealed a significant reduction in the ratio of time spent in open vs closed arm in AD group, when compared with control (p= 0.0066) and sham (p= 0.0081) groups at 60th day follow-up (fig.4.C.).

Moreover, qualitative analysis of anxiety of video track as representative of animal's exploratory movement in the EPM arena showed that the movement of AD group of rats was restricted more to the closed alley over open alley (fig.4.D.).

Change in ethograms of streptozotocin treated animals to anxiety like behaviour

Apart from the within and between group analysis of EPM paradigm, separately we have looked into the strategic changes if taken by the animals at the 60th day post-injection of STZ plotting the visual maps corresponding to the individual animals/ group. Therefore, the post-hoc videos of the terminal day were examined and tagged using kinoscope software where colour coding in the visual map of the Control and Sham group first of all showed an increased number of activity in form of crossing the five zones as compared to the AD group. Furthermore, in the control group we have observed more time spent in the open alley (north or south) labelled with black/red boxes especially in the 70% animals (C2-C6, C8-C9), which was accompanied by unprotected head dips (green bars). Whereas in case of the sham group we have found fraction of time spent/ exploration in open alley in the 54.5% animals (S1-S2, S5, S7-S9), again accompanied with green bars. Conversely, in case of the AD group of animals we have observed more fraction of time spent in close alley (east or west) labelled as yellow/blue boxes in 72.7% animals (A1-A6, A9, A11) and this behaviour was tightly associated with incomplete open arm entry denoted by red bars (fig.4.E.i-iii.). Therefore, after i.c.v. STZ treatment animals during a trial i.e. 300 second precisely changes its strategic plan to explore the open/ close arm and choses to spend more time in either of the closed arm grooming or prefer to transit from east to west closed arm or vice-versa immediately after an incomplete open arm entry while crossing through the central area or junction of the open and closed arm. Furthermore, 54.5% of animals in the AD group prefer to explore either of the closed arm after placing it on to the central area at the start point. At this initial moment of decisions, we have observed stretch-attend posture in majority of the AD induced animals. Taking together the quantitative and ethological variables it is evident that AD group of animals became more conscious/ alert while exploring the EPM arena and always have a self-check during transition from one arm to other. This can be best explained by cost-benefit model where animals prefer not to be active/ inquisitive to avoid anxiety burden.

Morphometric changes in the sub-regions of dorsal hippocampus of streptozotocin injected rat

As hippocampal neurodegeneration is one of the vital reason for cognitive decline therefore first of all, we measured the thickness of the layers juxtaposed to the CA1 sub region of hippocampus in all three experimental groups. We found a layer-wise atrophy in the thickness starting from stratum oriens layer (Or) to the infrapyramidal blade of dentate gyrus (IPBDG) after STZ treatment which has been illustrated superimposed on the cresyl violet stained image (fig.5.A.).

Next, we examined third ventricular volume enlargement through the Calivery procedure in cresyl violet stained sections. Where, Kruskal-Wallis statistics revealed a significant change across the group ($p=0.0005$; df= 2; KW= 11.43) and Dunn's multiple comparison test exhibited an significant increase in third ventricle of AD group as compared to Control ($p=0.014$) and Sham ($p=0.007$) group (fig.5.E.i.). Then, we have measured CA1 layer thickness, and statistical analysis found significant change in left ($p= 0.0011$; df= 2; KW= 10.78) as well as right ($p= 0.0006$; df= 2; KW= 11.38) in Kruskal-Wallis test. Dunn's multiple comparison revealed significant reduction in AD group as compared to Control (right: $p= 0.009$; left: $p= 0.014$) and Sham (right: $p= 0.011$; left: $p= 0.012$) group. Furthermore, when CA3 layer thickness was examined we found a significant change in both right ($p= 0.0014$; df= 2; KW= 10.50) as well as left ($p= 0.0004$; df= 2; KW= 11.56) hemisphere. In Dunn's multiple comparison we found

a significant loss in thickness of CA3 layer in AD group as compared to Control (right: p= 0.041; left: p= 0.020) Sham (right: p= 0.006; left: p= 0.005) group of animals (fig.5.C.i-iv.). On 60th day post-STZ treatment, two-way ANOVA revealed significant influence of cell type ($p<0.0001$; df= 2; F=38.98); treatment ($p<0.0001$; df= 2; F= 243.2) and even interaction between two (p= 0.0039; df=2; F= 6.358) in left hippocampus. Similarly, significant influence of cell type ($p<0.0001$; df= 1; F= 33.09); treatment ($p<0.0001$; df= 2; F= 257.2) and even interaction between two (p= 0.0008; df=2; F= 8.475) was observed in right hippocampus. In both right and left hippocampus, Tukey's multiple comparison revealed a significant reduction of neuronal area both in CA1 as well as in CA3 layer of AD group as compared to control ($p<0.0001$) and sham ($p<0.0001$) group (fig.5.C.v-vi.).
A statistically significant ($p<0.0001$; df= 2; KW= 30.17) difference among the groups was observed on the cell count of CA1 layer as revealed by Kruskal-Wallis test. Multiple group comparison with Dunn's test revealed a significant ($p<0.0001$) reduction in the cell count in AD group as compared to all other group of rats. In case of CA3 layer, cell count also differed significantly ($p<0.0001$; df= 2; KW= 30.35) among the experimental groups and Dunn's multiple comparison revealed a significant reduction ($p<0.0001$) in AD group as compared to other groups (fig.5.E.ii-iii.). All these morphometric quantification results suggest degeneration of CA1 as well as CA3 layer of pyramidal cells in hippocampus of i.c.v. STZ treated rats at 60th day post injection.
Further, we also checked for lateralization or hemispheric-biasness if any, for the neuronal area in two hippocampi. Two-way ANOVA analysis showed significant influence of brain areas/ cell types ($p<0.0001$; df= 3; F= 21.48), treatment/ groups ($p<0.0001$; df= 2; F= 553.6) and interaction between the two (p=0.0004; df= 6; F= 4.425). However, multiple comparison with Tukey's test did not show any significant change either in CA1 or in CA3 sub region of hippocampus between the two hemispheric data in any of the experimental groups studied (fig.5.F.).

Detection of congophilic particles in the brain of streptozotocin injected rats

Upon evaluation of Congo-red stained samples, we observed congophilic extracellular amyloid plaque deposited in the CA3 sub region of hippocampus of i.c.v. STZ treated rats at 60th day (fig. 6.A.vi.), whereas, in control and sham groups we did not find any such deposits in any region of the brain. Further, when other brain areas of the AD group were examined, similar deposits were present in the striatal region and caudate putamen (fig. 6.B.i-iii.). In addition, these deposits were found in both the hemispheres, which has been illustrated in fig. 6.C, spanning an area of 3.27mm in AP axis. These findings underpin that the cognitive impairments observed in behaviour or the neural loss in hippocampus in AD group might be tightly related to the deposition of Aβ plaque in various brain areas on 60th day post i.c.v. STZ injection.

Neuronal and spine morphology of granular cells in streptozotocin injected rats

In order to understand the synaptic plasticity in the polymorphic layer of hippocampus we had measured the neurite length, soma perimeter, spine density of the granular cells after Golgi-Cox staining at the end of the study period (fig. 6.D.i-iii.). Ordinary ANOVA test we found no change (p= 0.225; df= 2; KW= 3.035) in the neurite length across the groups. However, significant changes were observed in the soma perimeter ($p<0.0001$; df= 2; F= 32.94), where Bonferroni's multiple comparison revealed a significant reduction in AD group ($p<0.0001$) as compared to other counterparts. Furthermore, spine density were found to be significantly changed across the group ($p<0.0001$; df= 2; F= 74.09) and multiple comparison exhibited a significant reduction in the AD group ($p<0.0001$) as compared to others (fig. 6.D.iv.-vi.; E.).

Subcellular localization of GSK3ß, mtCOX-1 and PI3K in the limbic system of streptozotocin injected rats

When we compared the adjacent sections of CA1 pyramidal layer of dorsal hippocampus (at -4.36mm) we found more number of GSK3β$^+$ cells across the whole stratum pyramidale layer (marked with arrow)in AD group. Even in the CA3 layer, we found more expression of GSK3β$^+$ cells in AD group as compared to that of Control and Sham counterpart. However, comparison of CA1 and CA3 layer showed elevated expression of GSK3β$^+$ cells in CA3 layer with comparison to CA1 layer in AD group. Further, when we looked into the amygdala juxtaposed to piriform cortex and claustrum (at AP -2.28mm), expression of GSK3β$^+$ was much lesser in all the sections of Control and Sham group of rats, whereas, the expression was significantly more in the AD group. Similar increase in the GSK3β$^+$ cells was also found hypothalamic region juxtaposed to third ventricles in AD group (at AP-2.28mm), and septum (at AP-0.24mm) or more specifically bed nucleus of stria terminalis in comparison to Control and Sham group (fig. 7.A: 1.a.-5.c.).

Further, on comparison of the sections stained with anti-mtCOX and anti-PI3K antibody, we found an upregulation of mt-COX in the stratum pyramidale and stratum lacunosum layer of CA1 subfield of hippocampus in Control as well as Sham group, whereas it was downregulated in the i.c.v. STZ treated rats. Similarly, in CA3 we found a downregulation of mt-COX protein in AD group and in other two groups the expression was more in the stratum orience and stratum pyramidale. We also observed less expression of mt-COX in amygdala of AD group as compared to Control and Sham group. Then, in hypothalamus (AP -2.28mm) and in septum (AP -0.24mm) we saw a similar upregulation of mt-COX$^+$ cells expanding in all the layers of the mentioned brain area in Control and Sham group, on contrary, AD group revealed a downregulation of the same (fig. 7.B; C: 1.a.-5c.). Taken together, these results were represented in the fig. 7.D.i-ii. with both illustrating the expression pattern of three different markers as well as mean intensity profile in nested graph for insulin signalling and mitochondrial activity in five different brain areas after on 60th day of STZ treatment.

Correlation between the morpho-functional variables

Finally in order to understand and predict the exact mechanism of action of STZ for the cognitive and neuropsychiatric changes seen in the present study we have performed pairwise correlation between the behavioural and other variables in python. Statistical analysis showed that there are strong correlation between the morphometric and immune parameter studied in the ICV-STZ injected rat brain with their behavioural execution. These correlation showed proved that findings in the functional (memory and anxiety domain) experiments are tightly related/ associated with the morphological (histometric and subcellular expression of markers) variables on the 60th day post injection, as shown in the correlation heatmap with correlation coefficient values and heat map scale (fig. 8.A.). Further, we have performed regression analysis and plotted it between those variables which were found to be more prominently related to each other. There also we have seen the similar association between either morpho-functional or morpho-morpho variables (fig. 8.B.). From these correlation results we have illustrated the predicted mechanism of action of streptozotocin injection intracerebroventricularly in male Wistar rats on 60th day (Fig. 8.C.).

Discussions

We have observed a loss of spatial, episodic and avoidance memory in progressive manner from 15th day to the 60th day post-injection of STZ. Further, intergroup comparison revealed this impairment in memory domains are also remain same as compared to that of control and sham operated groups, suggesting a cognitive decline after ICV-STZ injection at 3mg/kg.

Further, multivariate analysis of distribution of fraction of time spent in four quadrants of MWM tank on 60th day post-injection of STZ revealed that loss in spatial memory causes changes in swimming strategy, which is similar to that of new learner. This showed that long term memory loss in this animal model is affecting the retention of spatial memory. Bilateral as well as unilateral single or two doses have been shown to induce severe progressive cognitive impairments. Examination of spatial and reference memory in MWM and elevated plus maze for 14 weeks after i.c.v. STZ injection revealed a slow and progressive loss of cognition from two weeks onwards (Mehla et al., 2013; Moreira-Silva et al., 2018). Cognitive impairment seen in 3mg/Kg i.c.v. STZ injection was associated with overexpression of cytokines at 15th, 18th, 21st day post-injection as assessed with radial arm maze for working and reference memory (Ghosh et al., 2020). In elevated plus maze, a reduction of transfer latency was reported on 17th, 18th, 19th day following twice STZ injection and was found to be correlated with elevation of reactive oxygen species and lipid peroxidation (Kamat et al., 2016; Sharma and Gupta, 2001).

Unilateral STZ treatment in the left lateral ventricle of WT female mice is shown to have severe loss of episodic memory, which was similar to that of triple transgenic mice model of AD (Chen et al., 2013). In the same study, the recognition memory deficits seen on 14th day post-injection were associated with dysfunction in insulin signaling pathway proteins along with synaptic protein downregulation. In another study by the same group, using unilateral model of STZ injection and 3xTg model, showed elevation in the expression of 84 genes associated with APP processing, microtubule associated protein tau, synaptic protein, apoptosis/ autophagy, glucose metabolism and mTOR pathway in both the models to a similar extent (Chen et al., 2012). These changes were reported to funnel down the cognitive impairment shown after six weeks of STZ injection. Murtishaw et al., (2018) showed that even systemic administration of STZ at 40mg/kg body wt. on 1, 2, 3, 14, 15 day lead to significant impairment in the discrimination between novel and familiar object exploration, suggesting a neurodegeneration similar to AD and vascular type dementia (Murtishaw et al., 2018). Our results of OTORT experiments also showed a progressive loss of episodic memory at each follow-up time points in AD group as compared to the Sham and Control group. In a recent study, Moreira-Silva et al., (2018) reported loss of short term recognition memory on 30th day post injection of STZ, which was associated with loss of synaptic proteins in hippocampus and enlargement of lateral ventricles (Moreira-Silva et al., 2018). When Wistar rats were tested for object recognition memory after 8th and 14th week post-injection they showed memory deficit along with upregulation in the phosphor-tau/ tau ratio in the hippocampus (Gáspár et al., 2021). An interesting finding in this paper was that Wistar rats were more prone to have AD like pathological phenotype when compared to the Long-Evans rats. Thus, substantiating evidence that selection of right strain for toxin based animal models of human disease is very important. When STZ treated rats were investigated for a stretch of 9 months post-injection for avoidance memory, a slow but steady cognitive deficit in 3mg/kg of body wt. rats was observed exhibiting a biphasic pattern (Knezovic et al., 2015). The pattern of cognitive performance of i.c.v. STZ treated animals showed an immediate severe loss after one week of STZ treatment but an increase on 3rd and decreases from 6 -9 month post-injection, the reason was speculated to have an immediate ROS, RNS insult induced by STZ. Though this study focused on long term consequences of STZ injection on cognitive function and pathological staging, they missed out on the time period between 2 weeks- 3 months, which according to other studies is the most crucial period wherein severe cognitive as well as morphological deficits are manifested. Further to get a complete picture of the avoidance memory domain in AD, number of error committed should also have been considered. In our results, we found a severe decline in avoidance memory in PASD test as reflected by step down latency and number of errors at every follow-up time-points starting from 15th day post injection of STZ until 60 days with no

biphasic pattern. When single injection of STZ at 3mg/kg of body wt. was administered then a decrease in the avoidance memory in AD group was reported on 14th, 21st and 18th day post injection as compared to control group. This cognitive decline was associated with oxidative stress responses and loss of cholinergic nerve fibers (Mehla et al., 2012b). However, Gáspár et al., (2021) observed avoidance memory at 6th and 11th week post twice (2x1.5mg/kg) or thrice injections (3x1.5mg/kg) of STZ in lateral ventricle and reported no significant change either in step through latency or number of error at any of the follow-up periods (Gáspár et al., 2021). They used shuttle box to study passive avoidance at 6th and 11th week and also gave twice or thrice STZ at a much lower dose of 1.5mg/kg, which may not have been sufficient dosage to induce damage that could result in impairment of avoidance memory.

Next, we had looked into the anxiety level in ICV-STZ injected rats, which is seen to be progressively increasing as reflected by decrease in head dipping duration. However, between group comparison showed a significant anxiety only at the 60th day post-injection of ICV-STZ. In the same experiment ethogram analysis using kinoscope revealed that 72.7% of animals showed an anxious phenotype with spending more time in the close alley of EPM. Again here in this test we have observed a change in the strategy of animals induced AD with ICV-STZ avoiding to be inquisitive to suppress the anxiety burden. Even, there were more incomplete transition/ entry in the open arm from the close in these animals suggesting a fearful response making them more conscious of their behavioural execution. Chen et al., (2013) also showed an anxiogenic effect in i.c.v unilateral STZ treated rats on 21st day post-injection, however they used female mice and earlier experimental evidences has reported effect of sex difference on cognitive function (Chen et al., 2013). Further, no available literature investigated the risk assessment behavior as characterized by head dipping in elevated plus maze. In our results, head dipping duration was found to be reduced with time in AD group, confirming acrophobia induced anxiety in AD. Even a low dose of 1.5mg/kg of body wt. STZ injection in lateral ventricles of mice showed anxiogenic effect in EPM on 7th as well as 21st day post-injection (Pinton et al., 2011). In knock-in model of AD 3xTg female mice enhanced levels of anxiety and fear was observed as assessed by startle responses, freezing behavior and increased restlessness, suggesting an association of neuropsychological behavioral phenotype akin to that seen in human patients (Sterniczuk et al., 2010).

Cognitive impairment in the AD patient or animal models have been directly associated with the neurodegeneration in the dorsal hippocampus (Fuster-Matanzo et al., 2011; Maruszak et al., 2014; O'Callaghan et al., 2019). In present study, we have found apreciable neurodegeneration in ICV-STZ injected group were more restricted to the dorsal hippocampus (fig. 5.E.). This led us to perform histometry of the hippocampus and associated structures viz. layerwise thickness near to dCA1, morphometry and cell density of CA1 and CA3 layer and third ventricular volume, which showed a neurodegeneration and third ventricular enlargement on 60th day post-injection of STZ. Though inter-hemispheric comparison did not show any lateral biasness. During spatial navigation or exploring novel environment, pyramidal neurons of CA1 and CA3 develop place fields, spatially selective firing fields of place cells, which play an important role in encoding spatial memories. Loss of these neurons leads to spatial memory deficits, as also observed in the present study. In a clinical study where Nissl stained sections were compared for CA1-CA4 of AD brain and age-matched control, prominent neuronal loss was seen only in the CA1 and CA3 pyramidal cell layer of hippocampus, indicating sensitivity of these areas in AD (Padurariu et al., 2012). West et al., (2004) also reported significant neuronal loss in CA1 subfield of hippocampus (48%) as compared other regions; hilus (14%) and subiculum (24%) in AD patients postmortem brain, though in pre-clinical AD cases no significant changes were observed in any of the areas (West et al., 2004). Twice injection (2x1.5mg/kg body wt.) of STZ is reported to have fluoro-Jade C positive cells in CA1 subfield of hippocampus, indicating neuronal degeneration (Yuliani et al., 2020). STZ treatment at a

dose of 3mg/kg of body wt. revealed a loss of intact neurons in CA1 pyramidal cell layer on 22nd day post-injection under Cresyl violet staining (Ahmed et al., 2013). Further even gestational systemic administration of STZ at diabetic dose showed a reduction in the density of neurons in CA1 and CA3 but no change in the thickness of the same layers on postnatal 7th and 21st day (Golalipour et al., 2012), confirming neurodegeneration in CA1 and CA3 layers of hippocampus as the hallmark of AD.

A substantial number of reports have demonstrated the presence of amyloid plaques after third month of STZ treatment either by single or twice injection model in various brain areas like hippocampus, cortex, striatum, even in the meningeal capillaries using congo-red, thioflavin-S and $A\beta_{1-42}$ antibody staining (Afshar et al., 2018; Knezovic et al., 2015; Salkovic-Petrisic et al., 2011). Hippocampal homogenate of i.c.v. STZ treated rats also showed elevated expression of $A\beta_{1-42}$ by ELISA or western blot technique from 30th day post-injection (Ahn et al., 2020; Azadfar et al., 2020; Bao et al., 2017; Shalaby et al., 2019). Only in one report reported diffuse amyloid deposition by congored staining on 30th day post injection of STZ though in this study authors did not focused on the hippocampus proper or related structures (Gupta et al., 2018). On examination of coronal sections with Congo-red staining, deposition of congophilic particle at 60th day post-injection was evident in CA3 layer of hippocampus, cingulate gyrus, primary motor cortex and corpus callosum. We did not observe amyloid deposits in capillaries or blood vessels as we speculate that these plaques are first manifested in insulin signaling imbalance prone brain areas and then with disease progression, they traverse through the cerebral meninges showing diffuse and extensive deposition of amyloids more globally, as seen in the present study.

Synaptic dysfunction is one of the cause of cognitive decline seen in sporadic AD. Dentate gyrus is known to be the site of neural pluripotent stem cells and this can be the region for adult neurogenesis. Neuroanatomical organization of dentate gyrus possess an unidirectional afferent fibre towards CA3 layer of hippocampus called mossy fibre tightly associated with episodic memory (Amaral et al., 2007). Experimental body of evidences mainly focused on the CA1 subfield of dorsal hippocampus of human patients (Padurariu et al., 2012). In the present study we had examined the spine morphology of the granular cells and its neurite length, which is found to be damaged on the 60th day of the ICV-STZ injection. This suggests synaptic dysfunction in the dentate gyrus, site for neurogenesis reflecting a sporadic form of AD. In previous series of paper on STZ induced rat model of diabetes mellites (type I) showed loss of spine in prefrontal cortex, occipital cortex and hippocampus, further more specifically they have showed that this loss in hippocampus is not only restricted to the CA1 pyramidal neurons but also dentate gyrus granular cells and these changes were also extended to dendritic level. In their second paper they have reported to reverse the condition after cerebrolysin administration (Martínez-Tellez et al., 2005; Sanchez-Vega et al., 2015). Further in another article these changes were found to be similar to the AD like pathology, which is tightly associated with Aβ1-42 in frontal cortex and hippocampus (Wang et al., 2014). In one recent paper combination of Golgi-Cox and methoxy-X04 staining in APP/PS1 mouse showed dendritic trimming and spine loss vicinity to amyloid plaques (Kartalou et al., 2020). Another report on 6 month old APP/PS1 mouse model of AD from Christophe Mulle's group showed that episodic memory deficit in these animals were associated with decrease in LTP with downscaling of spine of mossy fiber from dentate gyrus to CA3 layer of hippocampus (Viana Da Silva et al., 2019). On the other hand in another article authors showed synaptic sysfunction along with amyloidopathy when STZ is injected into the cisterna magna of rodents at 3mg/kg of body weight (Ahn et al., 2020). In line with that, we have observed a strong correlation between the episodic memory variable versus spine density in granular cells of dentate gyrus in ICV-STZ injected rats.

Further, to understand the details of energy metabolism in the STZ treated rats after 60th day post injection we have stained the coronal sections with anti-GSK3β, anti-mt-COX1 antibody and anti-PI3K, which are involved in TCA-cycle or electron transport in mitochondrial membrane and neuronal survival respectively. Immunostaining showed an upregulation of the GSK3β and downregulation of mt-COX in the brain areas of limbic system of AD group as compared to Control and Sham group. Unilateral injection of 3mg/kg i.c.v. STZ was found to increase expression of GSK3β in gene as well as protein level at 21st day post-injection in hippocampus and frontal cortex, associated with cognitive and neuropsychiatric dysfunction (Chen et al., 2013, 2012). They also observed imbalance in MAP kinase, PI3K, AKt, presenilin I and BAX, suggesting an insulin signaling dysfunction in the hippocampus as well as frontal cortex. When hippocampal cell line HT-22 was treated with STZ then apart from apoptotic, tau hyperphosphorylation and synaptic loss, Drp1, a mitochondrial fission protein was found to be over expressed suggesting mitochondrial fragmentation (Park et al., 2020). Even transmission electron microscopic and mitochondrial membrane potential measurement studies showed evidence on alterations in mitochondrial ultrastructure, decrease in transmembrane potential, repolarization level and ATP content after i.c.v. STZ injection (C. Correia et al., 2013; Knezovic et al., 2015; Salkovic-Petrisic et al., 2013).
These results suggest significant slow and progressive cognitive impairment after intracerebroventricular STZ injection due to neurodegeneration, amyloid deposition and mitochondrial dysfunction.

Acknowledgements:
We acknowledge the central animal facility of All India Institute of Medical Sciences, New Delhi for providing animals in the present study. We acknowledge Mr Sanjeev Beniwal (Department of Physiology, AIIMS, New Delhi) for assistance in behavioral experiment and Dr Priyanka Kumari (histology facility, Departent of Physiology, All India Institute of Medical Sciecnes, New Delhi) for assistance in histology. **Funding:** this work is supported by institutional fund from AIIMS, Ministry of Human Resource Development and Indian Council for Medical Research (IR-594/2019/RS). **Author Contributions:** AR and SJ has conceived the idea and planned the experiment; AR written the manuscript with suggestion from SJ, JK, TCN; JK and YKG supervised cognitive behavioral testing and drug administration, dose selection; TCN supervised histological experiment; SS has conducted Dirichlet distribution and kinoscope analysis with suggestion from AR; experiments were carried out and data curated by AR and SS; AR performed stereotaxic surgeries and tissue isolation; immunostaining was performed by AR and SS; histometric and other image analysis was performed by AR.

Competing interests:
The authors declare that the research was conducted in the absence of any commercial or financial relationships that could be construed as a potential competing of interest.

Data availability:
Raw data analyzed in the present study will be available with request to lead contact.

Reference:

Afshar, S., Shahidi, S., Rohani, A.H., Komaki, A., Asl, S.S., 2018. The effect of NAD-299 and TCB-2 on learning and memory, hippocampal BDNF levels and amyloid plaques in Streptozotocin-induced memory deficits in male rats. Psychopharmacology (Berl). 235, 2809–2822. https://doi.org/10.1007/s00213-018-4973-x

Ahmed, M.E., Moshahid Khan, M., Javed, H., Vaibhav, K., Khan, A., Tabassum, R., Ashafaq, M., Islam, Farah, Safhi, M.M., Islam, Fakhrul, 2013. Amelioration of cognitive impairment and neurodegeneration by catechin hydrate in rat model of streptozotocin-induced experimental dementia of Alzheimerâ€™s type. Neurochem. Int. 62, 492–501. https://doi.org/10.1016/j.neuint.2013.02.006

Ahn, Y., Seo, J., Park, J., Won, J., Yeo, H.-G., Kim, K., Jeon, C.-Y., Huh, J.-W., Lee, S.-R., Lee, D.-S., Lee, Y., 2020. Synaptic loss and amyloid beta alterations in the rodent hippocampus induced by streptozotocin injection into the cisterna magna. Lab. Anim. Res. 36. https://doi.org/10.1186/s42826-020-00049-x

Amaral, D.G., Scharfman, H.E., Lavenex, P., 2007. The dentate gyrus: fundamental neuroanatomical organization (dentate gyrus for dummies). Prog. Brain Res. 163. https://doi.org/10.1016/S0079-6123(07)63001-5

Azadfar, P., Noormohammadi, Z., Noroozian, M., Eidi, A., Mortazavi, P., 2020. Effect of memantine on expression of Bace1-as and Bace1 genes in STZ-induced Alzheimeric rats. Mol. Biol. Rep. 47, 5737–5745. https://doi.org/10.1007/S11033-020-05629-7

Bao, J., Mahaman, Y.A.R., Liu, R., Wang, J.-Z., Zhang, Z., Zhang, B., Wang, X., 2017. Sex Differences in the Cognitive and Hippocampal Effects of Streptozotocin in an Animal Model of Sporadic AD. Front. Aging Neurosci. 9. https://doi.org/10.3389/fnagi.2017.00347

Blokland, A., Jolles, J., 1993. Spatial-Learning Deficit and Reduced Hippocampal Chat Activity in Rats after an Icv Injection of Streptozotocin. Pharmacol. Biochem. Behav. 44, 491–494. https://doi.org/10.1016/0091-3057(93)90497-H

Bott, R., 2014. Bancroft's Theory & Practice of Histological Techniques; 7th ed, Igarss 2014. https://doi.org/10.1007/s13398-014-0173-7.2

C. Correia, S., X. Santos, R., S. Santos, M., Casadesus, G., C. LaManna, J., Perry, G., A. Smith, M., I. Moreira, P., 2013. Mitochondrial Abnormalities in a Streptozotocin-Induced Rat Model of Sporadic Alzheimer's Disease. Curr. Alzheimer Res. https://doi.org/10.2174/1567205011310040006

Chen, Liang, Z., Blanchard, J., Dai, C.L., Sun, S., Lee, M.H., Grundke-Iqbal, I., Iqbal, K., Liu, F., Gong, C.X., 2013. A non-transgenic mouse model (icv-STZ mouse) of Alzheimer's disease: similarities to and differences from the transgenic model (3xTg-AD mouse). Mol. Neurobiol. 47, 711–725. https://doi.org/10.1007/s12035-012-8375-5

Chen, Tian, Z., Liang, Z., Sun, S., Dai, C. ling, Lee, M.H., LaFerla, F.M., Grundke-Iqbal, I., Iqbal, K., Liu, F., Gong, C.X., 2012. Brain Gene Expression of a Sporadic (icv-STZ Mouse) and a Familial Mouse Model (3xTg-AD Mouse) of Alzheimer's Disease. PLoS One 7, 1–12. https://doi.org/10.1371/journal.pone.0051432

Ebel, D.L., Torkilsen, C.G., Ostrowski, T.D., 2017. Blunted Respiratory Responses in the Streptozotocin-Induced Alzheimer's Disease Rat Model. J. Alzheimer's Dis. 56, 1197–1211. https://doi.org/10.3233/JAD-160974

Efird, J., 2011. Blocked randomization with randomly selected block sizes. Int. J. Environ. Res. Public Health 8, 15–20. https://doi.org/10.3390/ijerph8010015

El Sayed, N.S., Ghoneum, M.H., 2020. Antia, a Natural Antioxidant Product, Attenuates Cognitive Dysfunction in Streptozotocin-Induced Mouse Model of Sporadic Alzheimer's Disease by Targeting the Amyloidogenic, Inflammatory, Autophagy, and Oxidative Stress Pathways. Oxid. Med. Cell. Longev. 2020.

https://doi.org/10.1155/2020/4386562
Ennaceur, A., Delacour, J., 1988. A new one-trial test for neurobiological studies of memory in rats. 1: Behavioral data. Behav. Brain Res. https://doi.org/10.1016/0166-4328(88)90157-X
Ferry, B., Gervasoni, D., Vogt, C., 2014. Stereotaxic neurosurgery in laboratory rodent: Handbook on best practices, Stereotaxic Neurosurgery in Laboratory Rodent: Handbook on Best Practices. https://doi.org/10.1007/978-2-8178-0472-9
Filho, G.L.B., Zenki, K.C., Kalinine, E., Baggio, S., Pettenuzzo, L., Zimmer, E.R., Weis, S.N., Calcagnotto, M.E., De Souza, D.O., 2015. A new device for step-down inhibitory avoidance task - Effects of low and high frequency in a novel device for passive inhibitory avoidance task that avoids bioimpedance variations. PLoS One. https://doi.org/10.1371/journal.pone.0116000
Fronza, M.G., Baldinotti, R., Martins, M.C., Goldani, B., Dalberto, B.T., Kremer, F.S., Begnini, K., Pinto, L. da S., Lenardão, E.J., Seixas, F.K., Collares, T., Alves, D., Savegnago, L., 2019. Rational design, cognition and neuropathology evaluation of QTC-4-MeOBnE in a streptozotocin-induced mouse model of sporadic Alzheimer's disease. Sci. Rep. 9, 1–14. https://doi.org/10.1038/s41598-019-43532-9
Fuster-Matanzo, A., Llorens-Martín, M., Barreda, E.G. de, Ávila, J., Hernández, F., 2011. Different Susceptibility to Neurodegeneration of Dorsal and Ventral Hippocampal Dentate Gyrus: A Study with Transgenic Mice Overexpressing GSK3β. PLoS One 6, e27262. https://doi.org/10.1371/JOURNAL.PONE.0027262
Gage, G.J., Kipke, D.R., Shain, W., 2012. Whole Animal Perfusion Fixation for Rodents. JoVE (Journal Vis. Exp. e3564. https://doi.org/10.3791/3564
Gáspár, A., Hutka, B., Ernyey, A.J., Tajti, B.T., Varga, B.T., Zádori, Z.S., Gyertyán, I., 2021. Intracerebroventricularly Injected Streptozotocin Exerts Subtle Effects on the Cognitive Performance of Long-Evans Rats. Front. Pharmacol. 0, 1130. https://doi.org/10.3389/FPHAR.2021.662173
Ghosh, R., Sil, S., Gupta, P., Ghosh, T., 2020. Optimization of intracerebroventricular streptozotocin dose for the induction of neuroinflammation and memory impairments in rats. Metab. Brain Dis. 35, 1279–1286. https://doi.org/10.1007/s11011-020-00588-1
Golalipour, M.J., Kafshgiri, S.K., Ghafari, S., 2012. Gestational diabetes induced neuronal loss in CA1 and CA3 subfields of rat hippocampus in early postnatal life. Folia Morphol. 71.
Grünblatt, E., Salkovic-Petrisic, M., Osmanovic, J., Riederer, P., Hoyer, S., 2007. Brain insulin system dysfunction in streptozotocin intracerebroventricularly treated rats generates hyperphosphorylated tau protein. J. Neurochem. 101, 757–770. https://doi.org/10.1111/j.1471-4159.2006.04368.x
Gupta, S., Yadav, K., Mantri, S.S., Singhal, N.K., Ganesh, S., Sandhir, R., 2018. Evidence for Compromised Insulin Signaling and Neuronal Vulnerability in Experimental Model of Sporadic Alzheimer's Disease. Mol. Neurobiol. 55, 8916–8935. https://doi.org/10.1007/S12035-018-0985-0
Hoyer, S., 2002. The aging brain. Changes in the neuronal insulin/insulin receptor signal transduction cascade trigger late-onset sporadic Alzheimer disease (SAD). A mini-review. J. Neural Transm. https://doi.org/10.1007/s007020200082
Hoyer, S., 2000. Brain glucose and energy metabolism abnormalities in sporadic Alzheimer disease. Causes and consequences: An update, in: Experimental Gerontology. https://doi.org/10.1016/S0531-5565(00)00156-X
Hoyer, S., 1998. Is sporadic Alzheimer disease the brain type of non-insulin dependent diabetes mellitus? A challenging hypothesis. J. Neural Transm. https://doi.org/10.1007/s007020050067

Kamat, P.K., 2015. Streptozotocin induced Alzheimer's disease like changes and the underlying neural degeneration and regeneration mechanism. Neural Regen. Res. 10, 1050. https://doi.org/10.4103/1673-5374.160076

Kamat, P.K., Kalani, A., Rai, S., Tota, S.K., Kumar, A., Ahmad, A.S., 2016. Streptozotocin Intracerebroventricular-Induced Neurotoxicity and Brain Insulin Resistance: a Therapeutic Intervention for Treatment of Sporadic Alzheimer's Disease (sAD)-Like Pathology. Mol. Neurobiol. https://doi.org/10.1007/s12035-015-9384-y

Kartalou, G.I., Endres, T., Lessmann, V., Gottmann, K., 2020. Golgi-Cox impregnation combined with fluorescence staining of amyloid plaques reveals local spine loss in an Alzheimer mouse model. J. Neurosci. Methods 341. https://doi.org/10.1016/J.JNEUMETH.2020.108797

Knezovic, A., Osmanovic-Barilar, J., Curlin, M., Hof, P.R., Simic, G., Riederer, P., Salkovic-Petrisic, M., 2015. Staging of cognitive deficits and neuropathological and ultrastructural changes in streptozotocin-induced rat model of Alzheimer's disease. J. Neural Transm. 122, 577–592. https://doi.org/10.1007/s00702-015-1394-4

Kokras, N., Baltas, D., Theocharis, F., Dalla, C., 2017. Kinoscope: An open-source computer program for behavioral pharmacologists. Front. Behav. Neurosci. 11, 88. https://doi.org/10.3389/FNBEH.2017.00088/BIBTEX

Kraska, A., Santin, M.D., Dorieux, O., Joseph-Mathurin, N., Bourrin, E., Petit, F., Jan, C., Chaigneau, M., Hantraye, P., Lestage, P., Dhenain, M., 2012. In Vivo Cross-sectional Characterization of Cerebral Alterations Induced by Intracerebroventricular Administration of Streptozotocin. PLoS One 7, 1–9. https://doi.org/10.1371/journal.pone.0046196

Lin, L.F., Jhao, Y.T., Chiu, C.H., Sun, L.H., Chou, T.K., Shiue, C.Y., Cheng, C.Y., Ma, K.H., 2022. Bezafibrate Exerts Neuroprotective Effects in a Rat Model of Sporadic Alzheimer's Disease. Pharmaceuticals 15. https://doi.org/10.3390/ph15020109

Liu, H., Zhong, L., Dai, Q., Yang, J., Zhang, Y., Zhang, B., Jiang, Y., 2022. Zuoguiwan Ameliorates Cognitive Deficits and Neuro-Inflammation in Streptozotocin-Induced Alzheimer's Disease Rats. Neuroimmunomodulation 29, 63–69. https://doi.org/10.1159/000516396

Martínez-Tellez, R., Gómez-Villalobos, M.D.J., Flores, G., 2005. Alteration in dendritic morphology of cortical neurons in rats with diabetes mellitus induced by streptozotocin. Brain Res. 1048, 108–115. https://doi.org/10.1016/J.BRAINRES.2005.04.048

Maruszak, A., Thuret, S., Mueller, S.G., Boccia, M.M., 2014. Why looking at the whole hippocampus is not enough-a critical role for anteroposterior axis, subfield and activation analyses to enhance predictive value of hippocampal changes for Alzheimer's disease diagnosis. Front. Cell. Neurosci. 8. https://doi.org/10.3389/fncel.2014.00095

Maugard, M., Doux, C., Bonvento, G., Morris, R.G.M., 2019. new statistical method to analyze Morris Water Maze data using Dirichlet distribution [version 2 ; peer review : 2 approved]. F1000Research 8, 1–14.

Mehla, J., Pahuja, M., Dethe, S.M., Agarwal, A., Gupta, Y.K., 2012a. Amelioration of intracerebroventricular streptozotocin induced cognitive impairment by Evolvulus alsinoides in rats: In vitro and in vivo evidence. Neurochem. Int. 61, 1052–1064. https://doi.org/10.1016/J.NEUINT.2012.07.022

Mehla, J., Pahuja, M., Dethe, S.M., Agarwal, A., Gupta, Y.K., 2012b. Amelioration of intracerebroventricular streptozotocin induced cognitive impairment by Evolvulus alsinoides in rats: In vitro and in vivo evidence. Neurochem. Int. 61, 1052–1064. https://doi.org/10.1016/J.NEUINT.2012.07.022

Mehla, J., Pahuja, M., Gupta, Y.K., 2013. Streptozotocin-induced sporadic Alzheimer's Disease: Selection of appropriate dose. J. Alzheimer's Dis. https://doi.org/10.3233/JAD-

2012-120958
Moreira-Silva, D., Carrettiero, D.C., Oliveira, A.S.A., Rodrigues, S., dos Santos-Lopes, J., Canas, P.M., Cunha, R.A., Almeida, M.C., Ferreira, T.L., 2018. Anandamide Effects in a Streptozotocin-Induced Alzheimer's Disease-Like Sporadic Dementia in Rats. Front. Neurosci. 0, 653. https://doi.org/10.3389/FNINS.2018.00653
Morris, R., 1984. Developments of a water-maze procedure for studying spatial learning in the rat. J. Neurosci. Methods. https://doi.org/10.1016/0165-0270(84)90007-4
Murtishaw, A., Heaney, C., Bolton, M., Belmonte, K., Langhardt, M., Kinney, J., 2018. Intermittent streptozotocin administration induces behavioral and pathological features relevant to Alzheimer's disease and vascular dementia. Neuropharmacology 137, 164–177. https://doi.org/10.1016/J.NEUROPHARM.2018.04.021
O'Callaghan, C., Shine, J.M., Hodges, J.R., Andrews-Hanna, J.R., Irish, M., 2019. Hippocampal atrophy and intrinsic brain network dysfunction relate to alterations in mind wandering in neurodegeneration. Proc. Natl. Acad. Sci. 116, 3316–3321. https://doi.org/10.1073/PNAS.1818523116
Padurariu, M., Ciobica, A., Mavroudis, I., Fotiou, D., Baloyannis, S., 2012. HIPPOCAMPAL NEURONAL LOSS IN THE CA1 AND CA3 AREAS OF ALZHEIMER'S DISEASE PATIENTS. Psychiatr. Danub. 24, 152–158.
Park, J., Won, J., Seo, J., Yeo, H.-G., Kim, K., Kim, Y.G., Jeon, C.-Y., Kam, M.K., Kim, Y.-H., Huh, J.-W., Lee, S.-R., Lee, D.-S., Lee, Y., 2020. Streptozotocin Induces Alzheimer's Disease-Like Pathology in Hippocampal Neuronal Cells via CDK5/Drp1-Mediated Mitochondrial Fragmentation. Front. Cell. Neurosci. 14. https://doi.org/10.3389/fncel.2020.00235
Paxinos, G., Charles Watson, 2007. The Rat Brain in Stereotaxic Coordinates Sixth Edition, Elsevier Academic Press.
Pinton, S., da Rocha, J., Gai, B., Nogueira, C., 2011. Sporadic dementia of Alzheimer's type induced by streptozotocin promotes anxiogenic behavior in mice. Behav. Brain Res. 223, 1–6. https://doi.org/10.1016/J.BBR.2011.04.014
Ranjan, A., Mallick, B.N., 2010. A modified method for consistent and reliable Golgi-Cox staining in significantly reduced time. Front. Neurol. https://doi.org/10.3389/fneur.2010.00157
Rostami, F., Javan, M., Moghimi, A., Haddad-Mashadrizeh, A., Fereidoni, M., 2017. Streptozotocin-induced hippocampal astrogliosis and insulin signaling malfunction as experimental scales for subclinical sporadic Alzheimer model. Life Sci. 188, 172–185. https://doi.org/10.1016/j.lfs.2017.08.025
Roy, A., Nag, T.C., Gupta, Y.K., Jain, S., 2021. Extremely low intensity magnetic field effectively improves cognitive impairment in intracerebroventricular streptozotocin animal model sparing septo-hippocampal cholinergic pathway and CAMKII. Alzheimer's Dement. 17, e049698. https://doi.org/10.1002/ALZ.049698
Salkovic-Petrisic, Hoyer, S., 2007. Central insulin resistance as a trigger for sporadic Alzheimer-like pathology: An experimental approach. J. Neural Transm. Suppl. 217–233. https://doi.org/10.1007/978-3-211-73574-9-28
Salkovic-Petrisic, M., Knezovic, A., Hoyer, S., Riederer, P., 2013. What have we learned from the streptozotocin-induced animal model of sporadic Alzheimer's disease, about the therapeutic strategies in Alzheimer's research. J. Neural Transm. 120, 233–252. https://doi.org/10.1007/s00702-012-0877-9
Salkovic-Petrisic, M., Osmanovic-Barilar, J., Brückner, M.K., Hoyer, S., Arendt, T., Riederer, P., 2011. Cerebral amyloid angiopathy in streptozotocin rat model of sporadic Alzheimer's disease: A long-term follow up study. J. Neural Transm. 118, 765–772. https://doi.org/10.1007/s00702-011-0651-4

Salkovic-Petrisic, M., Tribl, F., Schmidt, M., Hoyer, S., Riederer, P., 2006. Alzheimer-like changes in protein kinase B and glycogen synthase kinase-3 in rat frontal cortex and hippocampus after damage to the insulin signalling pathway. J. Neurochem. 96, 1005–1015. https://doi.org/10.1111/j.1471-4159.2005.03637.x

Sanchez-Vega, L., Juárez, I., De Jesus Gomez-Villalobos, M., Flores, G., 2015. Cerebrolysin reverses hippocampal neural atrophy in a mice model of diabetes mellitus type 1. Synapse 69, 326–335. https://doi.org/10.1002/SYN.21819

Schindelin, J., Arganda-Carreras, I., Frise, E., Kaynig, V., Longair, M., Pietzsch, T., Preibisch, S., Rueden, C., Saalfeld, S., Schmid, B., Tinevez, J.Y., White, D.J., Hartenstein, V., Eliceiri, K., Tomancak, P., Cardona, A., 2012. Fiji: An open-source platform for biological-image analysis. Nat. Methods. https://doi.org/10.1038/nmeth.2019

Shalaby, M.A., Nounou, H.A., Deif, M.M., 2019. The potential value of capsaicin in modulating cognitive functions in a rat model of streptozotocin-induced Alzheimer's disease. Egypt. J. Neurol. Psychiatry Neurosurg. 2019 551 55, 1–13. https://doi.org/10.1186/S41983-019-0094-7

Sharma, Gupta, Y., 2001. Intracerebroventricular injection of streptozotocin in rats produces both oxidative stress in the brain and cognitive impairment. Life Sci. 68, 1021–1029. https://doi.org/10.1016/S0024-3205(00)01005-5

Song, J.Z., Cui, S.Y., Cui, X.Y., Hu, X., Ma, Y.N., Ding, H., Ye, H., Zhang, Y.H., 2018. Dysfunction of GABAergic neurons in the parafacial zone mediates sleep disturbances in a streptozotocin-induced rat model of sporadic Alzheimer's disease. Metab. Brain Dis. 33, 127–137. https://doi.org/10.1007/s11011-017-0125-y

Sterniczuk, R., Antle, M.C., Laferla, F.M., Dyck, R.H., 2010. Characterization of the 3xTg-AD mouse model of Alzheimer's disease: Part 2. Behavioral and cognitive changes. Brain Res. 1348, 149–155. https://doi.org/10.1016/J.BRAINRES.2010.06.011

Viana Da Silva, S., Zhang, P., Haberl, M.G., Labrousse, V., Grosjean, N., Blanchet, C., Frick, A., Mulle, C., 2019. Hippocampal mossy fibers synapses in CA3 pyramidal cells are altered at an early stage in a mouse model of Alzheimer's disease. J. Neurosci. 39, 4193–4205. https://doi.org/10.1523/JNEUROSCI.2868-18.2019

Walf, A.A., Frye, C.A., 2007. The use of the elevated plus maze as an assay of anxiety-related behavior in rodents. Nat. Protoc. https://doi.org/10.1038/nprot.2007.44

Wang, J.Q., Yin, J., Song, Y.F., Zhang, L., Ren, Y.X., Wang, D.G., Gao, L.P., Jing, Y.H., 2014. Brain aging and AD-like pathology in streptozotocin-induced diabetic rats. J. Diabetes Res. 2014. https://doi.org/10.1155/2014/796840

West, M.J., Kawas, C.H., Stewart, W.F., Rudow, G.L., Troncoso, J.C., 2004. Hippocampal neurons in pre-clinical Alzheimer's disease. Neurobiol. Aging 25, 1205–1212. https://doi.org/10.1016/J.NEUROBIOLAGING.2003.12.005

Xu, Z.-P., Li, L., Bao, J., Wang, Z.-H., Zeng, J., Liu, E.-J., Li, X.-G., Huang, R.-X., Gao, D., Li, M.-Z., Zhang, Y., Liu, G.-P., Wang, J.-Z., 2014. Magnesium Protects Cognitive Functions and Synaptic Plasticity in Streptozotocin-Induced Sporadic Alzheimer's Model. PLoS One 9, e108645. https://doi.org/10.1371/journal.pone.0108645

Yuliani, T., Lobentanzer, S., Klein, J., 2020. Central cholinergic function and metabolic changes in streptozotocin-induced rat brain injury. J. Neurochem. https://doi.org/10.1111/JNC.15155

Zaqout, S., Kaindl, A.M., 2016. Golgi-cox staining step by step. Front. Neuroanat. https://doi.org/10.3389/fnana.2016.00038

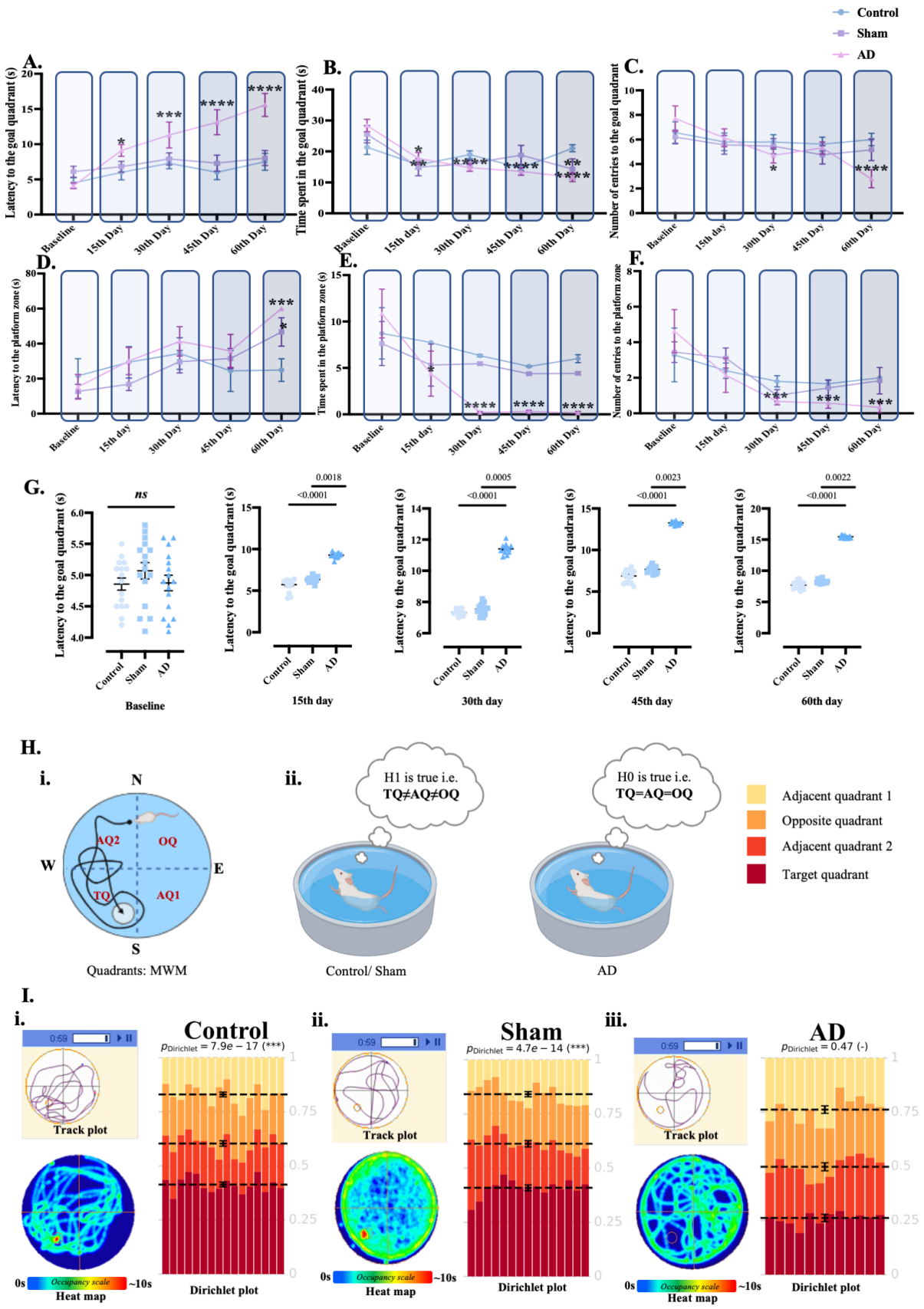

Figure 1.: Progressive loss of spatial memory with fraction of time spent in the each quadrant dose not showed an equal or uniform distribution except in AD group of animals as assessed by MWM paradigm.

Within group analysis of latency to the goal quadrant (A.); time spent in the goal quadrant (B.); number of entries to the goal quadrant (C.); latency to the platform zone (D.); time spent in the platform zone (E.); number of entries in the platform zone (F.); between group comparison of latency to the goal quadrant (G.); template for zone division in MWM tank with the alternative quadrant (AQ), opposite quadrant (OQ) and target quadrant (TQ) made using BioRender application (H.i.); representation of alternative (H1) and null hypothesis (H0) as used in Dirichlet distribution of fraction of time spent in four quadrants in three groups with the colour code used in Dirichlet plot for four quadrants (H.ii); track plot, heat map and dirichlet plot where each column represents a sample and each colour represents a quadrant. Mean values for the fraction of the time spent in each quadrant is represented by a dotted line and the error bars on the means are approximated with the inverse Fisher information of control (I.i), sham (I.ii) and AD (I.iii.) with $n \geq 9$; data is expressed as Mean ±SEM except in G, where it is given as Mean ±SEM along with individual data points. * indicates comparison with baseline pre-surgery data ****$p \leq 0.0001$, *** $p \leq 0.001$, ** $p \leq 0.01$, * $p \leq 0.05$.

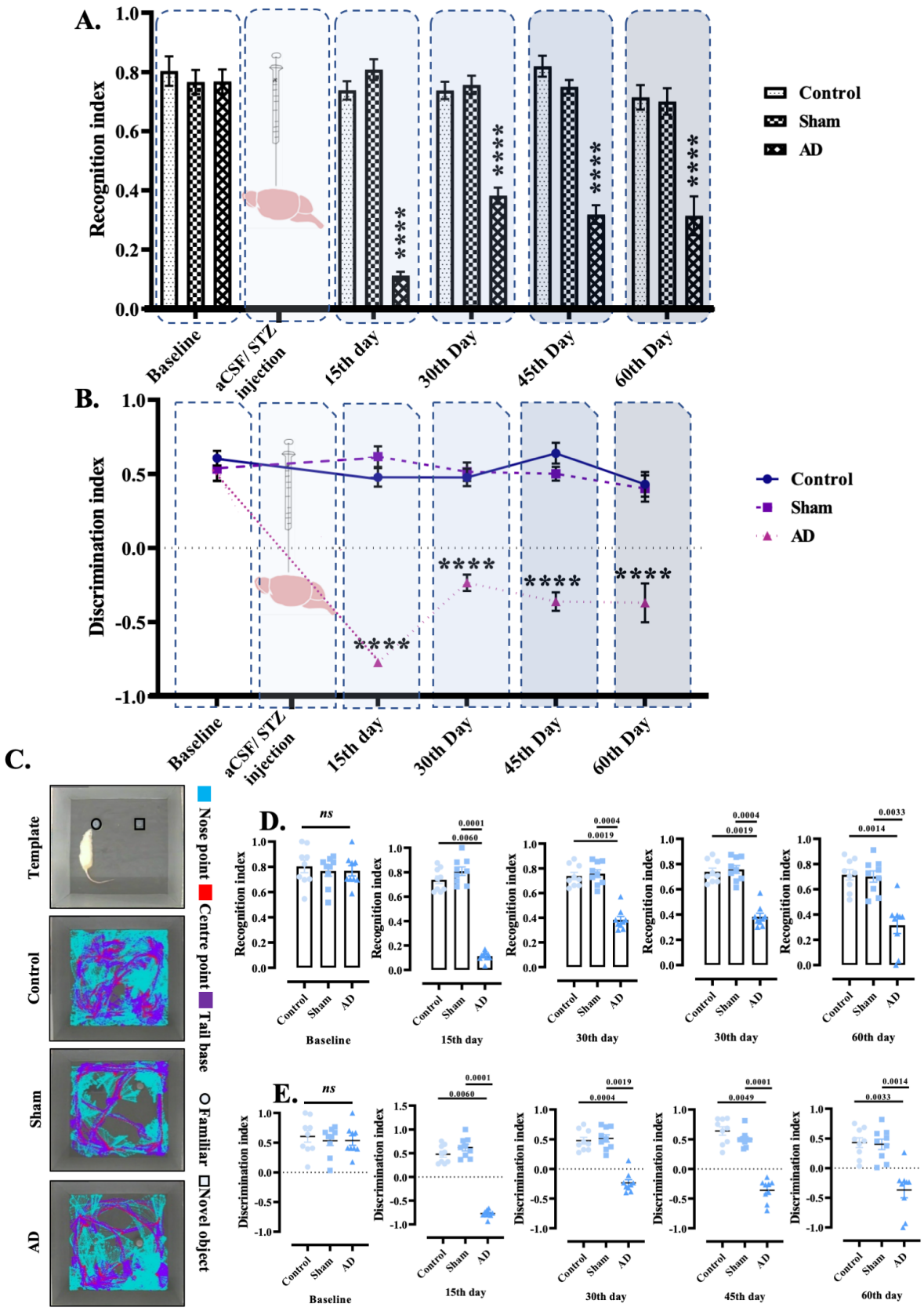

Figure 2.: Progressive loss of episodic memory post injection of streptozotocin as assessed by one trial object recognition paradigm.

within group analysis of recognition index (A.); and discrimination index (B.); track plot as well as template of the original recording frame (C.); between group analysis of recognition index (D.); and discrimination index at various study periods (E.) data is expressed as Mean ±SEM except in D. and E., where it is given as Mean ±SEM along with individual data points; * indicates comparison with baseline pre-surgery data; **** p≤ 0.0001; n≥9/ group.

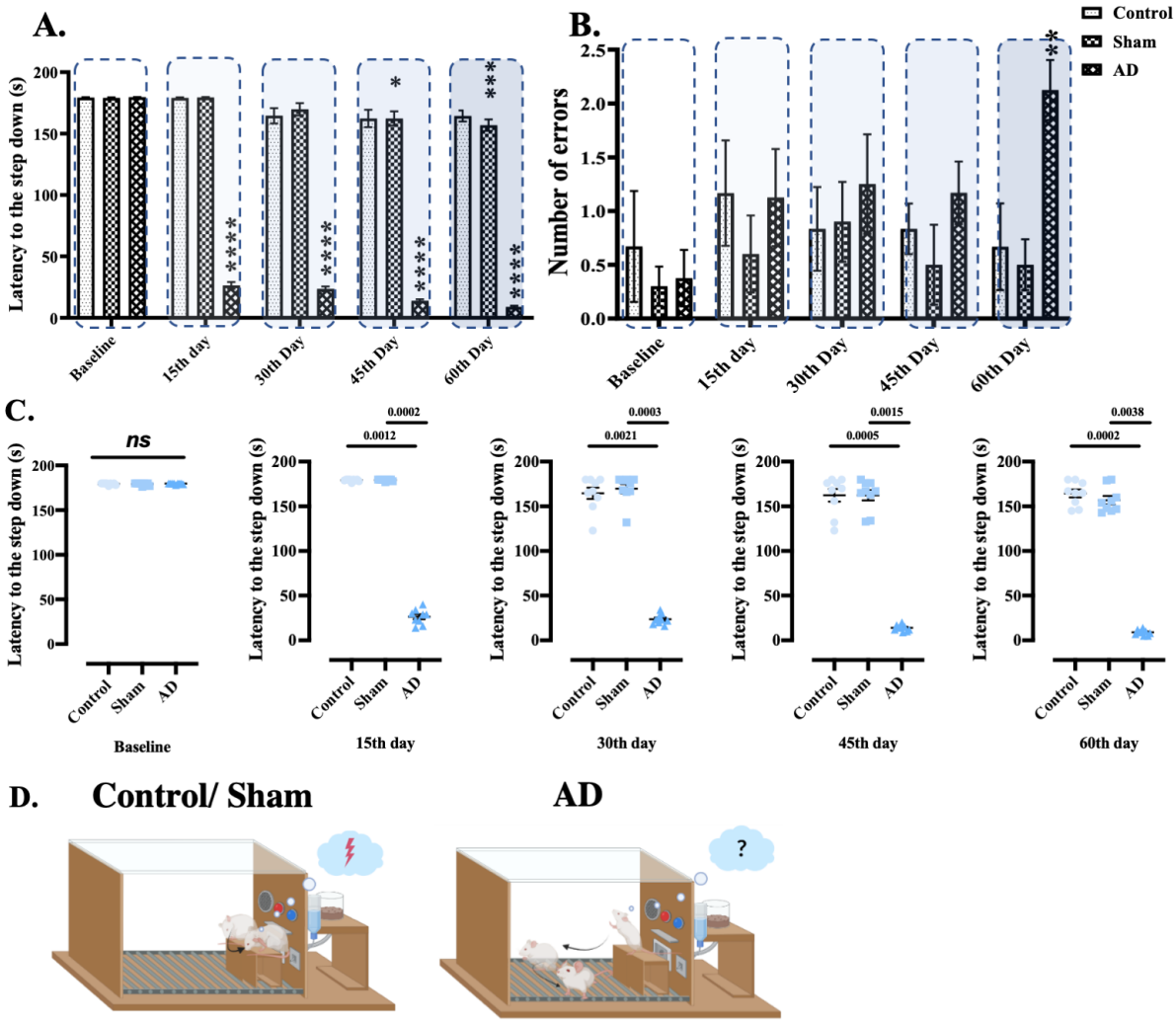

Figure 3.: Progressive loss of avoidance memory in streptozotocin induced AD rats as assessed by passive avoidance step-down paradigm.
within group analysis of latency to the step down (A.); and number of errors (B.); illustration of the control/sham group in upper panel and AD group in lower panel created in BioRender app(C.) between group analysis of latency to the step down (D.); data is expressed as Mean ±SEM except in D., where it is given as Mean ±SEM along with individual data points. *indicates comparison with baseline pre-surgery data ****p≤ 0.0001, ***p≤ 0.001, **p≤ 0.01.

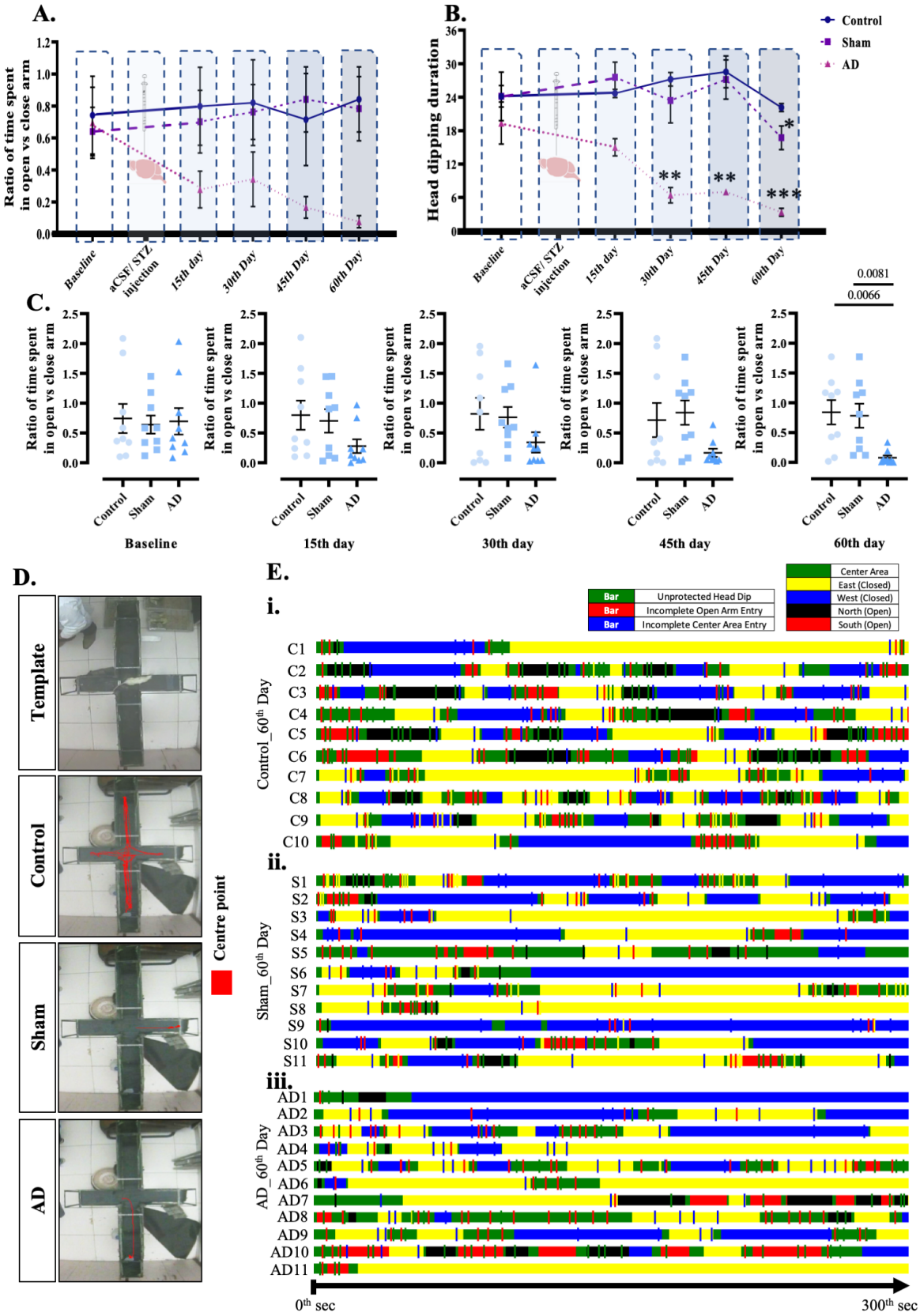

Figure 4.: Progressive increase in anxiety after streptozotocin injection with change in the strategy of exploration in elevated plus maze.

within group analysis of ratio of time spent in open vs closed arm (A.); and head dipping duration (B.); between group ratio of time spent in open vs closed arm (C.); representative track plot of experimental groups with template (D.); ethogram plotted along the time period of terminal behaviour recording on 60th day post-surgery where time spent is represented as column and activity in the arms were represented as bar in control (E.i.), sham (E.ii.), and AD (E.iii.) group; in the post-hoc ethogram analysis with kinoscope software time spent in center area (green), closed (east: yellow; west: blue) arm and open (north: black; south: red) arm are colour coded; data is expressed as Mean ±SEM except in C., where it is given as Mean ±SEM along with individual data points; * indicates comparison with baseline pre-surgery data *** $p \leq 0.001$, ** $p \leq 0.01$, * $p \leq 0.05$.

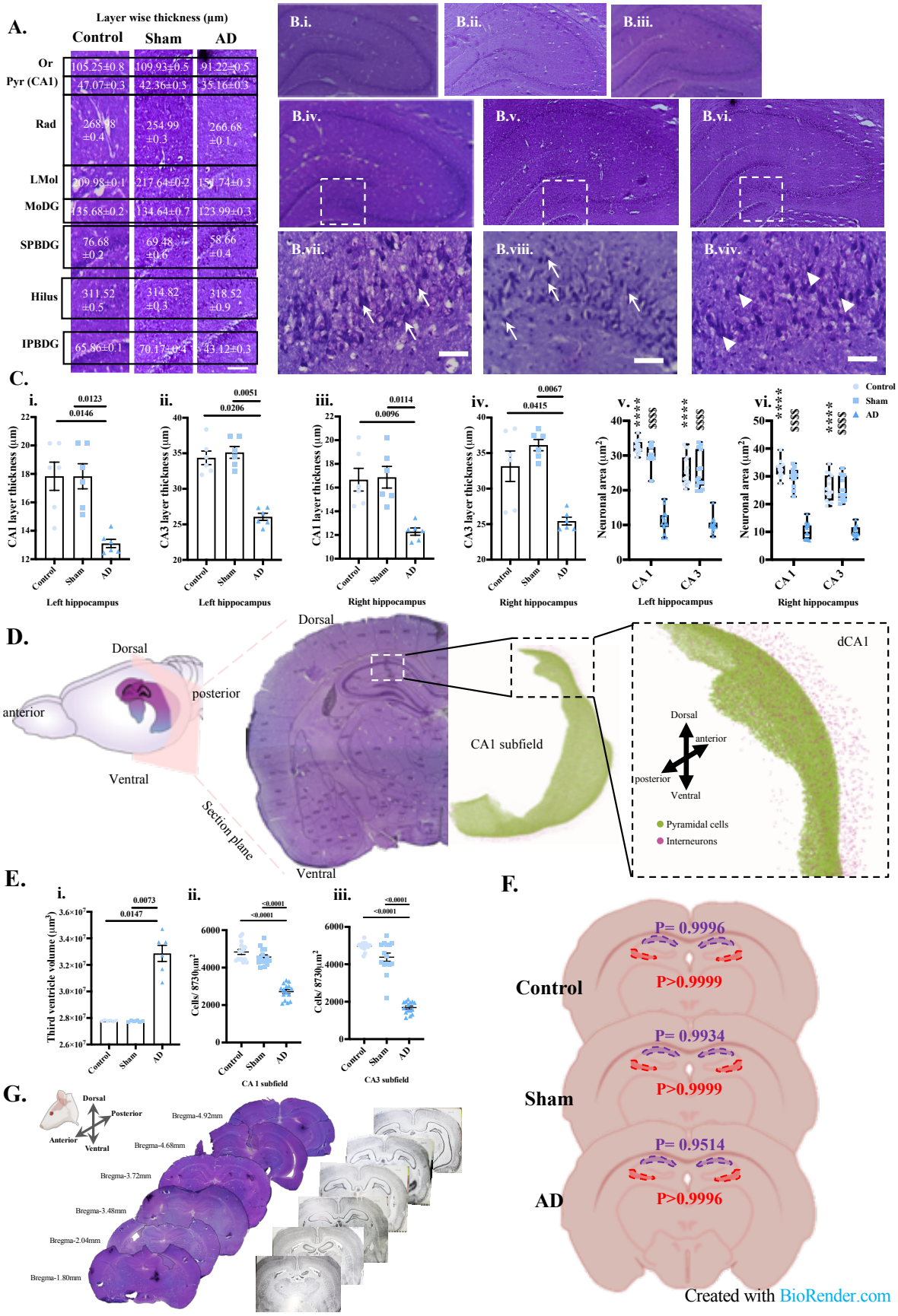

Figure 5.: Alteration in the cytoarchitecture of hippocampal sub regions with no lateral biasness and enlargement in cresyl violet stained coronal sections.

Layer wise thickness at the viscinity of the CA1 pyramidal layer of hippocampus (scale bar= 500µm; A.); photomicrograph of cresyl violet stained coronal section of Control rat at 4X, 20X and 40X (c.i., c.iv., c.vii.); Sham rat at 4X, 20X and 40X (c.ii., c.v., c.viii.); and AD rat at 4X, 20X and 40X (c.iii., c.vi., c.ix.) showing pycnotic cells with arrow head (scale bar= 50µm; B.); left hippocampal thickness of CA1 layer (C.i.), CA3 layer (C.ii.); right hippocampal thickness of CA1 (C.iii.), and CA3 (C.iv.) layer; neuronal area of left and right hippocampus (C.v-vi.); illustration representing coronal section showing the coronal plane marking the dorsal CA1 representing a detailed neuron model based on Ascoli atlas (https://pair-recording-bsp-epfl.apps.hbp.eu/circuits/rat-ca1) with pyramidal and interneuron (D.) third ventricular volume and cell count in CA1 and CA3 (E.i-iii.); hemispheric-biasness in different experimental groups (F.); selection of anterior-posterior plane to study alterations in AD group (G.); data in neuronal area is expressed as minimum and maximum with individual points whereas, cell count is expressed as Mean±SEM with individual data points; *denotes comparison between control and AD, $^{\$}$denotes comparison between sham and AD group; $^{****/\$\$\$\$}p \leq 0.0001$; n=3 with five fields at 40X magnification (15 data points/ group); or= stratum oriens, Pyr(CA1)= stratum pyramidale of CA1, Rad= stratum radiatum, LMol= lacunusum-moleculare, MoDG= molecular layer of dentate gyrus, SPBDG= suprapyramidal blade of dentate gyrus, IPBDG= infrapyramidal blade of dentate gyrus.

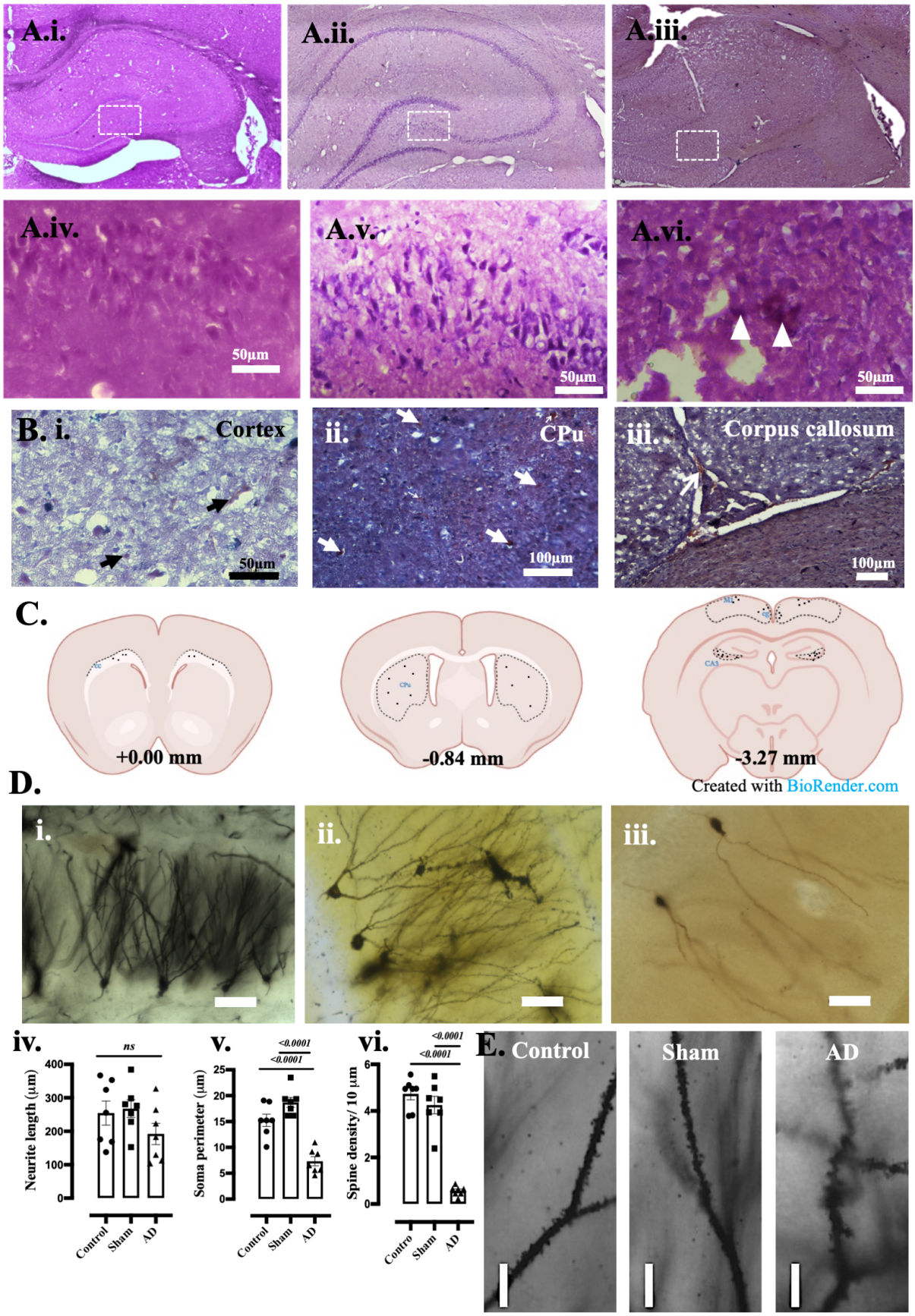

Figure 6.: Detection of amyloid plaque in hippocampal formation and impairment in synaptic plasticity in dentate gyrus of streptozotocin induced sporadic Alzheimer's disease.

Photomicrograph of Congo-red stained samples under lower (10X) and higher (40X) magnification of Control (A.i.; A.iv.), Sham (A.ii.; A.v.), and AD (A.iii.; A.vi.) group; Other areas of the brain in AD group showing presence of plaques (B.); schematic illustration of Aβ plaque in various coronal sections of brain of AD group with its AP axis made in BioRender (C.); Golgi-Cox stained granule cells of dendtate gyrus in control (D.i.), sham (D.ii.), and AD (D.iii.); neurite length (D.iv.), soma perimeter (D.v.), spine density (D.vi.) of granule cells; 100X magnification of spines at granule cells of dentate gyrus of contrl, sham and AD group (scale bar= 7µm; E.); Scale bar= as mentioned on the plates of Congo-red stained samples and 50µm in case of Golgi-Cox stained samples; M1= motor cortex; cg= cingulate gyrus; CPu= caudate putamen; cc= corpus callosum.

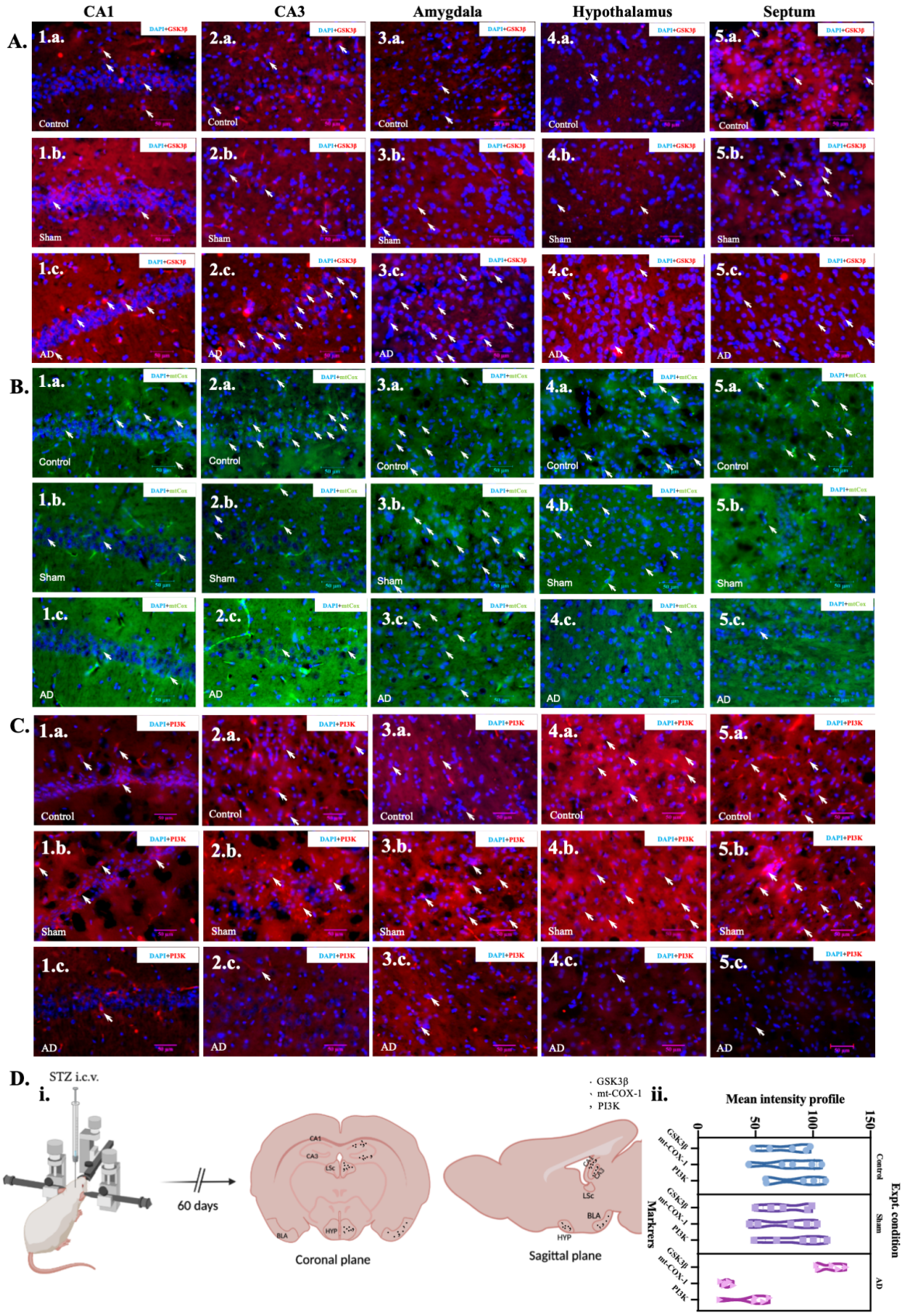

Figure 7.: Impairment in the insulin signalling and energy metabolism of brain areas associated with limbic system on two month post injection of streptozotocin.

Photomicrograph of immunostained sections of brain samples on 60th day post-injection of STZ for GSK3β (A.), mt-COX1 (B.), and PI3K (C.) counter stained with DAPI (in blue); 400X magnification images from Control, Sham and AD of CA1 (1.a-1.c.); CA3 (2.a.-2.c.); amygdala (3.a.-3.c.); hypothalamus (4.a.-4.c.); septum (5.a.-5.c.); study design for immunostaining illustrated along with the representative expression of three markers in coronal and sagittal plane of ICV-STZ injected rat (D.i.); mean intensity profile of the three markers are represented as nested plot with experimental groups (D.ii.); Data expressed as violin plot with individual values (n=5/group); CA1= cornuammnis 1, CA3= cornuammonis 3, LSc= lateral nucleus of septum, BLA= basolateral nucleus of amygdala, HYP= hypothalamus; scale bar= 50µm.

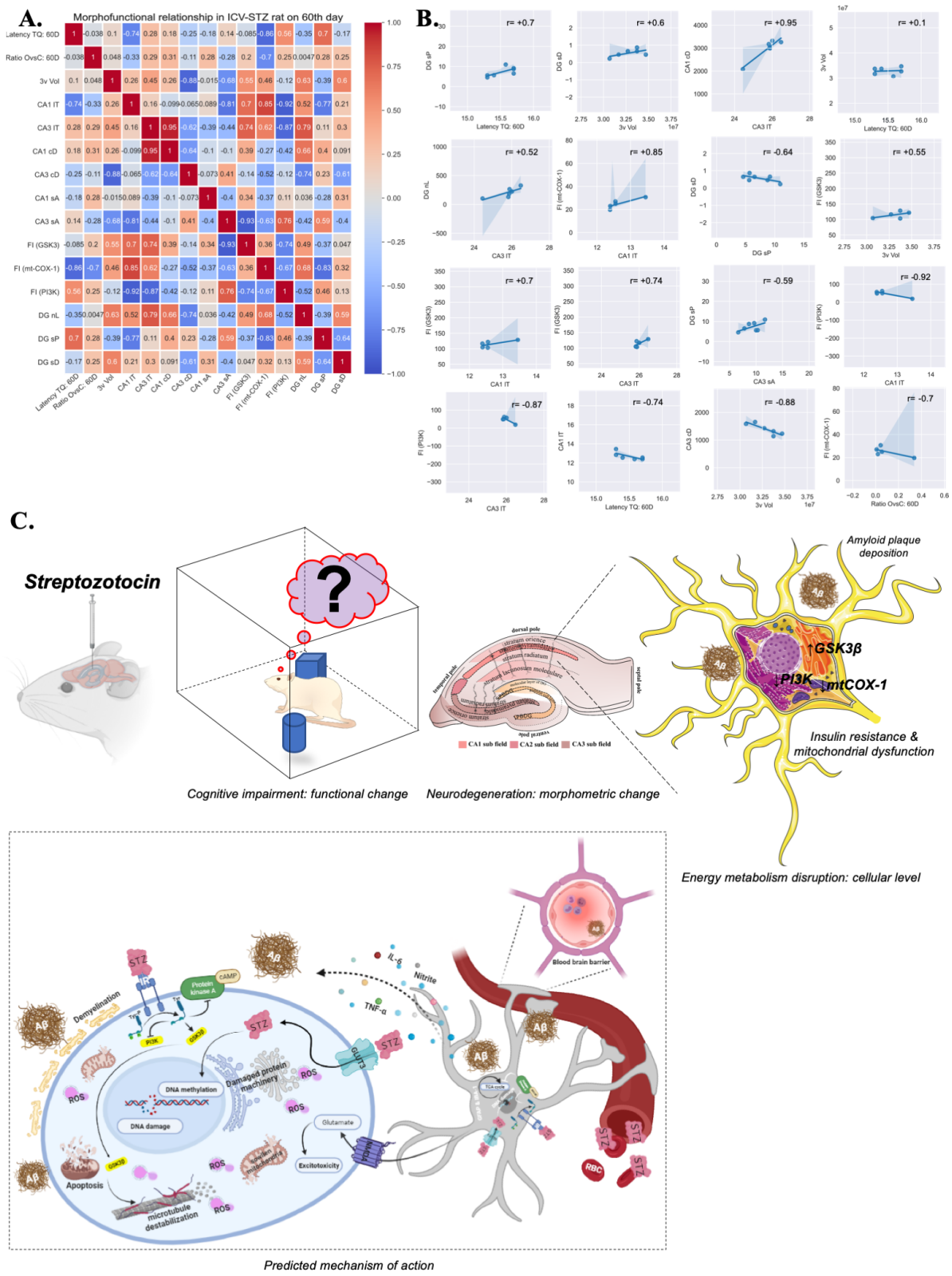

Figure 8.: Structure function relationship on 60th day in ICV-STZ injected rats.
Correlation matrix with the colour heatmap of ICV-STZ injected rats between functional and morphological variables (A.); reg-plot between important variable found to be strongly related in STZ induced AD rats (B.); proposed mechanism of action of streptozotocin when injected through lateral ventricles (made using BioRender and SMART ppt platform; C.).